

# The Long and Short of U.S. Treasury

Jun Liu, Jun Pan and Qing Peng\*

First draft: November 18, 2025. Current draft: June 11, 2026

## Abstract

We develop an arbitrage-free affine term-structure model to separately identify the *market-driven* long rate from the *policy-driven* short rate. Estimating this “long-short” model using term structures of zero-coupon yields, we show that the model provides a clean estimate of the latent long-rate component, in contrast to the commonly used 10-year yield, which blends both the short- and long-rate components. Focusing on the transmission of monetary policy shock (MPS), we find that, as expected, MPS transmits strongly to the short rate, while their impact on the latent long rate is muted. By contrast, using the 10-year forward yield as a proxy for the long rate, [Hanson and Stein \(2015\)](#) finds a significantly positive MPS amplification on the long rate. Our model can further decompose the term premium of [Adrian et al. \(2013\)](#) into risk premiums for the policy-driven short-rate risk and market-driven long-rate risk – we find that over 70 percent of the term premium can be attributed to the policy-driven duration risk. Moreover, the difference between the long and short rate – the slope of the term structure – functions as an important state variable for the market price of risk, increasing the term premium as the slope steepens.

---

\*Liu (junliu@ucsd.edu) is from the Rady School of Management at University of California San Diego; Pan (junpan@saif.sjtu.edu.cn) is from Shanghai Advanced Institute of Finance at Shanghai Jiao Tong University and Peng (qpeng@imf.org) is from International Monetary Fund Shanghai Center.

# 1 Introduction

The U.S. Treasury market lies at the center of the global financial system, providing the benchmark yield curve for asset valuation, guiding international capital allocation, and serving as the primary channel for monetary policy transmission. A fundamental question in this market centers on how changes in short-term interest rates propagate along the yield curve to affect long-term rates. This linkage is central to understanding how monetary policy shapes financial conditions, influences borrowing and investment decisions, and ultimately affects real economic activity.

While short-term interest rates are primarily policy-sensitive, directly influenced by the Federal Reserve’s rate decisions, long-term yields are largely market-driven, reflecting investors’ expectations about future economic and policy conditions. Importantly, movements in long rates can, in turn, shape policy choices by affecting financial conditions and the broader economy. A vivid example occurred in April 2025, when President Trump abruptly paused his sweeping tariff plan after a sharp sell-off in U.S. Treasuries drove the 10-year yield above 4.5%, triggering alarm across global markets and within the White House. As CNN reported<sup>1</sup>, the “bond vigilantes” effectively forced the administration to reverse course, illustrating how market-driven shifts in long rates can discipline fiscal and trade policy.

Distinguishing between short-rate and long-rate dynamics is essential for understanding monetary transmission, yet doing so empirically is challenging. The long-term yield observed in the market embeds expectations of future short rates as well as a time-varying term premium, making it difficult to separately identify policy-driven movements and market-driven components. To address this challenge, we develop a simple arbitrage-free “short catch long” affine term-structure model that separately identifies the latent short-rate factor capturing policy-sensitive variations and the latent long-rate factor reflecting market expectations. This framework provides a transparent and tractable way to quantify how changes in short-term interest rates propagate along the yield curve to affect long-term rates. More importantly, under the no-arbitrage affine term structure, we can write the term premium of long-term bonds as a linear function of our latent factors, allowing a clear analytical decomposition of yields into expected short rates and risk compensation. The decomposition also helps identify the distinct market and macroeconomic drivers of the two latent factors.

Our model builds on the affine term-structure framework that has become the workhorse of fixed-income research. Since the seminal work of [Duffie and Kan \(1996\)](#), researchers have modeled bond yields as exponential-affine functions of a small set of latent factors under the restriction of no arbitrage. Following this tradition, we propose a simple two-factor

---

<sup>1</sup><https://www.cnn.com/2025/04/11/business/bond-market-trump-treasury-yield-rates>

arbitrage-free model in which the short rate  $r_t$  mean-reverts toward a long-run component  $l_t$ , a mechanism we term “short catch long”. Unlike the two-factor Cox–Ingersoll–Ross (CIR) model of [Chen and Scott \(1992\)](#), our “long-short” specification assumes both factors follow Vasicek dynamics, providing analytical tractability while preserving rich interactions between the short- and long-term components.

By deriving the no-arbitrage cross-sectional pricing equation, we can write the yield on an  $n$ -period zero-coupon bond as an affine function of two latent state variables,  $x_t = (r_t, l_t)'$ :

$$y_t(n) = a(n) + b(n)'x_t.$$

This affine representation provides the basis for our estimation strategy. Traditional affine term-structure models are typically estimated by maximum likelihood or Kalman-filter-based maximum likelihood methods ([Dai and Singleton, 2000](#); [Duffee, 2002](#); [Kim and Orphanides, 2012](#)). [Adrian et al. \(2013\)](#), by contrast, propose a computationally efficient linear-regression approach that exploits the affine structure of bond yields to discipline both the time-series and cross-sectional dimensions of the term structure. Motivated by their approach, we estimate the long–short model using a two-stage regression-based procedure that separates risk-neutral pricing from physical factor dynamics.

In the first stage, we estimate the risk-neutral pricing parameters and recover the latent state variables from the cross section of zero-coupon yields. For any candidate set of  $\mathbb{Q}$ -measure parameters, the model-implied loadings  $a(n)$  and  $b(n)$  are known. Conditional on these loadings, the latent factors can be recovered at each date by projecting the observed cross section of yields onto the model-implied loadings. We then choose the  $\mathbb{Q}$ -measure parameters to minimize the sum of squared pricing errors across maturities and time. This stage identifies the risk-neutral pricing equation that best fits the yield curve and produces a time series of estimated latent factors  $\hat{x}_t^* = (\hat{r}_t, \hat{l}_t)'$ .

In the second stage, we estimate the physical dynamics of the latent factors. Taking the first-stage estimates  $\hat{x}_t^*$  as observed state variables, we fit the “short catch long” process under the physical measure. Because the continuous-time Gaussian dynamics imply a conditional normal distribution for  $\hat{x}_{t+1}^*$  given  $\hat{x}_t^*$ , the physical parameters are estimated by maximum likelihood. This step identifies the persistence and mean-reversion parameters governing the real-world evolution of the policy-sensitive short-rate component and the long-run rate component. The resulting procedure is transparent, computationally tractable, and consistent with the no-arbitrage affine structure.

*Latent Factors* – [Figure 1](#) plots the two latent state variables, the short rate  $r_t$  and the long-run mean  $l_t$ , extracted from the long–short model, alongside the fitted 3-month and 10-year zero-coupon yields. The implied short-rate factor  $r_t$  tracks monetary policy actions

closely, moving almost one-for-one with the 3-month yield and capturing the policy-sensitive component of the term structure. By contrast, the long-run factor  $l_t$  differs substantially from the observed 10-year yield. This divergence highlights why we need the long-short model to separately identify the long rate and the short rate. The market-observed 10-year yield cannot be treated as a clean proxy for the long rate because it represents a weighted average of both short- and long-term components. The long-short model provides a simple and transparent framework to separate these two forces. By isolating the policy-driven short-rate dynamics from the market-driven long-run expectations, the model enables us to quantify how changes in short-term rates or monetary policy shocks propagate through the yield curve and influence the latent long-run yield.

*Term Premium* – Another key output of the long-short model is the term premium, which represents the compensation investors require for holding long-term bonds rather than rolling over short-term bonds. In affine term-structure models, the term premium reflects the wedge between risk-neutral pricing and the physical expected path of future short rates. A key advantage of our framework is that this wedge can be expressed in closed form as a linear function of the two latent factors,

$$TP_t(n) = A(n) + B(n)r_t + C(n)l_t.$$

This representation allows us to directly trace how the policy-sensitive short-rate component and the market-driven long-rate component contribute to risk compensation at different maturities.

Our model estimates imply that the market price of short-rate risk in the long-short model is state dependent. The key state variable is the gap between the policy-sensitive short rate  $r_t$  and its long-run component  $l_t$ , which sheds light on the importance of the yield-curve slope. When  $r_t < l_t$ , which occurs during most normal times, long-term bonds are risky and investors require a higher term premium. The opposite case,  $r_t > l_t$ , is rare and often occurs before recessions. In this region, long-term bonds become better hedges, so the required term premium is lower. Holding the long-run component  $l_t$  fixed, an increase in  $r_t$  therefore moves the economy toward a region in which long-term bonds have stronger hedging value and require less risk compensation.

Consistent with this intuition, the estimated 10-year term premium loads negatively on the short-rate factor, with  $B = -0.44$ , and positively on the long-run factor, with  $C = 0.30$ . This pattern is consistent with the five-factor estimates of [Adrian et al. \(2013\)](#), in which term premia decline when expected short rates rise, and vice versa. We further decompose the 10-year term premium into model-implied sources of risk and find that it primarily compensates investors for policy-driven short-rate risk rather than market-driven long-rate risk.

Unlike much of the recent literature that explains term-premium movements through segmented investors, arbitrageur balance-sheet constraints, or rate-amplifying demand (Hanson et al., 2021; Kekre et al., 2024; Jansen et al., 2024; Vayanos and Vila, 2021), our approach takes a step back and considers a simple yet transparent arbitrage-free affine term-structure benchmark. The advantage of this benchmark is that the latent factors, the market price of risk, and the resulting term-premium loadings are analytically connected.

*Monetary Policy Shock* – Another application of the long-short model concerns the transmission of monetary policy to the long end of the yield curve. Two competing views about how monetary policy shocks affect long-term interest rates exist. The first emphasizes that a tightening (easing) shock should lead to a significant rise (decrease) in long-term yields. This view is formalized in models such as Jansen et al. (2024) and Kekre et al. (2024), which show that short-term rates influence long-term yields not only through expectations but also through the term premium. In these models, arbitrageurs play a critical role: when the Fed adopts tightening monetary policy, investors shift toward shorter maturities, forcing arbitrageurs to absorb more duration risk, which increases the term premium and amplifies the rise in long-term yields.

In contrast, the second theoretical camp suggests that long-term rates underreact to monetary policy shocks. This view is rooted in dynamic preferred-habitat models such as Vayanos and Vila (2021), where risk-averse arbitrageurs and maturity-specific bond demand jointly determine bond prices. Risk-averse arbitrageurs transmit shocks from the short-term interest rate to long-term rates through carry trades. However, because these arbitrageurs are not risk neutral, they limit their trades to manage interest-rate risk, which causes long-term rates to underreact to policy shocks.

In our long-short model, we back out the implied short rate  $r_t$  and the long-run mean  $l_t$  from the cross section of zero-coupon yields. Unlike prior studies that rely on observed 10-year yields (Gertler and Karadi, 2015; Gilchrist et al., 2015) or forward rates (Hanson and Stein, 2015), both of which mix implied short-rate and long-rate components, our model allows us to separately identify these effects cleanly. This decomposition allows us to assess the transmission of monetary policy shocks to the short and long ends of the yield curve with greater precision.

We identify monetary policy shocks using high-frequency changes in money-market futures around FOMC announcements, including the surprise component of federal funds futures from Kuttner (2001), the first four Eurodollar futures (ED1–ED4) from Bauer and Swanson (2022), and the target and path factors from Gurkaynak et al. (2005). Regressing the daily change in the implied short rate  $r_t$  and long-run mean  $l_t$  on these monetary surprises reveals a clear asymmetry: the short-rate factor responds strongly and significantly, while the long-run mean remains largely unaffected. A 100-basis-point increase in the current-

quarter Eurodollar surprise (ED1) raises the implied short rate  $r_t$  by about 63 basis points, yet produces no statistically significant change in the long-run component  $l_t$ . This pattern is robust across the market-based futures and Gurkaynak-Sack-Swanson target and path factors.

The weak response of  $l_t$  to these market-based surprises indicates that monetary policy shocks mainly shift near-term policy expectations without altering investors' perceptions of the long-run rate. In other words, the transmission of monetary policy operates almost entirely through the expectations channel. This stands in contrast to the accumulating empirical evidence that monetary policy shocks are amplified along the yield curve through movements in the term premium, in addition to their effects on expectations of future short rates (Gertler and Karadi, 2015; Gilchrist et al., 2015; Hanson and Stein, 2015; Hanson et al., 2021). The empirical results in our paper suggest that this amplification channel is weak: long-term yields are largely anchored by market expectations of future fundamentals rather than by short-term policy actions.

*Market and Macroeconomic Drivers* – Finally, we use the long-short decomposition to study what drives the two latent components outside monetary-policy event windows. This exercise provides an additional test of whether the latent factors have distinct economic content. If  $r_t$  captures the policy-sensitive short end of the curve, it should be closely related to variables that summarize near-term policy expectations, funding conditions, and short-rate movements. If  $l_t$  captures the market-driven long-rate component, it should instead comove with broader financial-market conditions, uncertainty, and macroeconomic fundamentals.

The evidence supports this interpretation. Both latent factors are positively related to S&P 500 returns and U.S. dollar movements, but the loading on the short-rate factor is substantially larger, especially for the dollar. Uncertainty variables further highlight the distinction between the two latent factors. VIX is negatively related to both  $r_t$  and  $l_t$ , consistent with broad risk-off episodes in which flight-to-safety forces lower the entire yield curve. By contrast, MOVE and economic policy uncertainty load mainly on  $l_t$ , suggesting that bond-market volatility and policy uncertainty are more closely associated with the market-driven long-rate component than with near-term policy-rate movements. Treasury-market liquidity measure by Hu et al. (2013), instead, loads primarily on  $r_t$ , pointing to a short-end liquidity or funding dimension.

As for macroeconomic fundamentals, core CPI inflation raises both the latent short-rate and long-rate factors, consistent with inflation increasing both near-term policy-rate expectations and the long-run nominal-rate anchor. The unemployment rate reveals the clearest difference between the two components. Higher unemployment lowers the short-rate factor, consistent with expected monetary easing, but raises the latent long-rate component, reflecting the pricing of longer-run macroeconomic risk and uncertainty. This relation is

obscured in the observed 10-year yield because the policy-driven short-rate effect and the market-driven long-rate effect offset each other. These results reinforce the central message of the long-short model: observed long-maturity yields mix economically distinct forces, and separating them reveals relationships that reduced-form yield regressions can miss.

*Related Literature* – Our paper builds on the large literature on affine term-structure models (ATSMs) that characterize bond yields as exponential-affine functions of a small set of latent factors under the restriction of no arbitrage. Early one-factor models such as [Vasicek \(1977\)](#) and [Cox et al. \(1985\)](#) were extended by [Duffie and Kan \(1996\)](#) and [Dai and Singleton \(2000\)](#), who formalized the general  $N$ -factor affine class and clarified its admissibility and identification conditions. Subsequent work improved empirical performance by relaxing restrictions on the market price of risk ([Duffee, 2002](#)), incorporating macroeconomic information into the pricing kernel ([Ang and Piazzesi, 2003](#)) and modeling stochastic volatility ([Cieslak and Povala, 2016](#)). [Joslin et al. \(2011\)](#) and [Christensen et al. \(2011\)](#) further connected affine models with the dynamic Nelson–Siegel representation, enhancing estimation tractability while preserving the no-arbitrage structure.

Our paper is also related to the growing literature on estimating the term premium component of long-term yields, which is the compensation investors demand for bearing interest-rate risk. Early empirical studies ([Kim and Orphanides, 2012](#); [Kim and Wright, 2011](#); [Kim and Orphanides, 2007](#)) estimate the U.S. Treasury term premium using no-arbitrage affine models augmented with survey expectations, highlighting the role of time-varying risk premia. Building on this approach, [Adrian et al. \(2013\)](#) propose a linear-regression-based five-factor affine model that efficiently estimates term premia using principal components of yields, which is widely employed in empirical research. [Hördahl and Tristani \(2018\)](#) incorporate macro factors in ATSMs and jointly model nominal and real yield curves with inflation expectations, finding that inflation risk premia are generally small and procyclical in the United States but countercyclical in the euro area. Our paper contributes to this literature by offering a simple and theoretically grounded affine framework in which the term premium is an explicit linear function of latent factors, enabling direct analysis of how short-rate dynamics influence the evolution of the term premium.

Finally, our paper is part of the literature on how short-term yields and monetary policy shocks transmit to the long end of the yield curve. Existing research emphasizes that monetary policy affects long-term yields not only through expectations of future short rates but also via movements in term premia. [Gertler and Karadi \(2015\)](#) show that policy tightening raises borrowing costs largely through higher term premia and credit spreads, highlighting the importance of financial frictions. [Hanson and Stein \(2015\)](#) find that contractionary policy shocks significantly increase long-term real forward rates, implying that term premia account for most of the response of long-term yields. [Hanson et al. \(2021\)](#) document an “excess sensi-

tivity” of long-term yields to short-term rate changes, suggesting that limited arbitrage and rate-amplifying investor demand cause long-term yields to overreact to short-rate changes. Building on these insights, [Vayanos and Vila \(2021\)](#) develop a preferred-habitat model where risk-averse arbitrageurs transmit short-rate shocks along the maturity spectrum, and [Kekre et al. \(2024\)](#) show that monetary tightening raises term premia when arbitrageur wealth is constrained. Recent evidence from [Jansen et al. \(2024\)](#) further demonstrates that heterogeneity in sector-level Treasury demand generates a downward-sloping term structure of market elasticity, consistent with long-term yields overreacting to policy shocks.

Our contribution is to provide a simple yet transparent no-arbitrage framework that estimates a latent long-rate factor  $l_t$  distinct from observed long-term yields. The estimated  $l_t$  differs substantially from the observed 10-year yield, underscoring that market yields cannot be treated as clean proxies for the long rate because they combine both policy-sensitive short-rate movements and market-driven long-rate variation.

A second contribution is to show that the market price of short-rate risk is state dependent in the long–short model. The relevant state variable is the gap between the policy-sensitive short rate  $r_t$  and its long-run component  $l_t$ . During most normal times,  $r_t < l_t$ , long-term bonds are risky and investors require a higher term premium. In the rare cases when  $r_t > l_t$ , often occurring before recessions, long-term bonds become better hedges and the required term premium is lower. This mechanism gives a simple risk-pricing interpretation to the countercyclical behavior of the term premium.

Consistent with this mechanism, we find that the 10-year term premium loads negatively on the short-rate factor and positively on the long-rate factor. The term premium therefore tends to decline when the policy-sensitive short rate rises, in line with the five-factor estimates of [Adrian et al. \(2013\)](#). Decomposing the term premium into model-implied risk sources further shows that the 10-year term premium primarily compensates policy-driven short-rate risk. Moreover, we show that monetary policy shocks mainly affect the short-rate component but have limited impact on the latent long-rate component, in contrast to much of the existing literature that relies on market-observed long-term yields such as the 10-year yield or forward rates.

Finally, we show that financial-market conditions and macroeconomic fundamentals load differently on the two latent factors: bond-market volatility, policy uncertainty, and unemployment are closely related to the market-driven long-rate component, while short-rate and funding conditions are more strongly reflected in the policy-sensitive short-rate factor.

## 2 The Long-Short Model

In this section, we set up the data-generating process for the arbitrage-free “short catch long” affine term-structure model and derive the no-arbitrage cross-sectional equation for bond yields. We then show how to estimate the model parameters via a two-stage regression-based procedure.

### 2.1 General Setup

#### 2.1.1 State Dynamics

Suppose there are two latent variables,  $r_t$  and  $l_t$ , under the data-generating process. The short rate  $r_t$  mean-reverts to the time-varying mean  $l_t$ , and the two factors satisfy

$$dr_t = -K_r(r_t - l_t)dt + \sigma_r dB_t \quad (1)$$

and

$$dl_t = -K_l(l_t - \bar{r})dt + \sigma_l(\rho dB_t + \sqrt{1 - \rho^2}dZ_t), \quad (2)$$

where  $(K_r, \sigma_r, K_l, \bar{r}, \sigma_l, \rho) \equiv \Theta$  are constant parameters. In matrix notation,

$$d \begin{pmatrix} r_t \\ l_t \end{pmatrix} = - \begin{pmatrix} K_r & -K_r \\ 0 & K_l \end{pmatrix} \begin{pmatrix} r_t - \bar{r} \\ l_t - \bar{r} \end{pmatrix} dt + \begin{pmatrix} \sigma_r & 0 \\ \rho\sigma_l & \sqrt{1 - \rho^2}\sigma_l \end{pmatrix} \begin{pmatrix} dB_t \\ dZ_t \end{pmatrix}. \quad (3)$$

We assume that the dynamics of  $r_t$  and  $l_t$  have the same diffusion structure but different drift parameters under the  $\mathbb{Q}$  measure:

$$dr_t = -K_r^{\mathbb{Q}}(r_t - l_t)dt + \sigma_r dB_t^{\mathbb{Q}} \quad (4)$$

and

$$dl_t = -K_l^{\mathbb{Q}}(l_t - \bar{r}^{\mathbb{Q}})dt + \sigma_l(\rho dB_t^{\mathbb{Q}} + \sqrt{1 - \rho^2}dZ_t^{\mathbb{Q}}), \quad (5)$$

where  $(K_r^{\mathbb{Q}}, \sigma_r, K_l^{\mathbb{Q}}, \bar{r}^{\mathbb{Q}}, \sigma_l, \rho) \equiv \Theta^{\mathbb{Q}}$  are constant parameters.

In matrix notation,

$$d \begin{pmatrix} r_t \\ l_t \end{pmatrix} = - \begin{pmatrix} K_r^{\mathbb{Q}} & -K_r^{\mathbb{Q}} \\ 0 & K_l^{\mathbb{Q}} \end{pmatrix} \begin{pmatrix} r_t - \bar{r}^{\mathbb{Q}} \\ l_t - \bar{r}^{\mathbb{Q}} \end{pmatrix} dt + \begin{pmatrix} \sigma_r & 0 \\ \rho\sigma_l & \sqrt{1 - \rho^2}\sigma_l \end{pmatrix} \begin{pmatrix} dB_t^{\mathbb{Q}} \\ dZ_t^{\mathbb{Q}} \end{pmatrix}. \quad (6)$$

### 2.1.2 Market Price of Risk

Let  $\lambda_{bt}$  and  $\lambda_{zt}$  denote the market price of risk for  $dB_t$  and  $dZ_t$  respectively,

$$\begin{pmatrix} dB_t \\ dZ_t \end{pmatrix} = \begin{pmatrix} dB_t^Q - \lambda_{bt}dt \\ dZ_t^Q - \lambda_{zt}dt \end{pmatrix} = \begin{pmatrix} dB_t^Q - (\lambda_b + \lambda_{br}r_t + \lambda_{bl}l_t)dt \\ dZ_t^Q - (\lambda_z + \lambda_{zr}r_t + \lambda_{zl}l_t)dt \end{pmatrix}. \quad (7)$$

The corresponding pricing kernel can be written as

$$\frac{dM_t}{M_t} = -r_t dt - (\lambda_b + \lambda_{br}r_t + \lambda_{bl}l_t) dB_t - (\lambda_z + \lambda_{zr}r_t + \lambda_{zl}l_t) dZ_t.$$

By Girsanov's theorem and matching constant terms, we can derive the following expressions for the market prices of risk:

$$\lambda_b = 0; \lambda_{br} = -\lambda_{bl} = \frac{K_r^Q - K_r}{\sigma_r}$$

$$\lambda_z = \frac{K_l \bar{r} - K_l^Q \bar{r}^Q}{\sqrt{1 - \rho^2} \sigma_l}; \lambda_{zr} = -\frac{\rho}{\sqrt{1 - \rho^2}} \lambda_{br}; \lambda_{zl} = \frac{1}{\sqrt{1 - \rho^2}} \left( \frac{K_l^Q - K_l}{\sigma_l} - \rho \lambda_{bl} \right)$$

### 2.1.3 Bond Yields

The term structure is completely determined by the risk-neutral parameters. The yield  $y_t(n)$  on an  $n$ -period zero-coupon bond at time  $t$  is given by

$$y_t(n) = \bar{r}^Q + (r_t - \bar{r}^Q) \frac{1}{n K_r^Q} (1 - e^{-K_r^Q n}) + (l_t - \bar{r}^Q) \frac{K_r^Q}{n(K_r^Q - K_l^Q)} \left( \frac{1}{K_l^Q} (1 - e^{-K_l^Q n}) - \frac{1}{K_r^Q} (1 - e^{-K_r^Q n}) \right)$$

$$- \frac{1}{2} \int_0^n \left( \frac{\sigma_r}{K_r^Q} (1 - e^{-K_r^Q(n-v)}) + \frac{\rho \sigma_l}{K_l^Q} (1 - e^{-K_l^Q(n-v)}) - \frac{\rho \sigma_l}{(K_r^Q - K_l^Q)} (e^{-K_l^Q(n-v)} - e^{-K_r^Q(n-v)}) \right)^2 \frac{dv}{n}$$

$$- \frac{1}{2} \int_0^n \frac{(1 - \rho^2) \sigma_l^2}{(K_r^Q - K_l^Q)^2} (e^{-K_l^Q(n-v)} - e^{-K_r^Q(n-v)})^2 \frac{dv}{n}.$$

The yield  $y_t(n)$  of maturity  $n$  at time  $t$  is

$$y_t(n) = a(n) + b(n)' x_t, \quad (8)$$

where  $x_t = (r_t, l_t)'$ , for  $n = 1, \dots, N$ . Given  $t$ ,  $x_t$  is a  $2 \times 1$  vector,  $y_t = (y_t(1), \dots, y_t(N))'$  is a  $N \times 1$  vector,  $a = (a(1), \dots, a(N))'$  is a  $N \times 1$  vector, and  $b = (b(1), \dots, b(N))'$  is a  $N \times 2$

matrix. The elements of  $a$  and  $b$  are

$$\begin{aligned}
a(n) &= \bar{r}^Q - \bar{r}^Q \frac{1}{nK_r^Q} (1 - e^{-K_r^Q n}) - \bar{r}^Q \frac{K_r^Q}{n(K_r^Q - K_l^Q)} \left( \frac{1}{K_l^Q} (1 - e^{-K_l^Q n}) - \frac{1}{K_r^Q} (1 - e^{-K_r^Q n}) \right) \\
&- \frac{1}{2} \int_0^n \left( \frac{\sigma_r}{K_r^Q} (1 - e^{-K_r^Q(n-v)}) + \frac{\rho\sigma_l}{K_l^Q} (1 - e^{-K_l^Q(n-v)}) - \frac{\rho\sigma_l}{(K_r^Q - K_l^Q)} (e^{-K_l^Q(n-v)} - e^{-K_r^Q(n-v)}) \right)^2 \frac{dv}{n} \\
&\quad - \frac{1}{2} \int_0^n \frac{(1 - \rho^2)\sigma_l^2}{(K_r^Q - K_l^Q)^2} (e^{-K_l^Q(n-v)} - e^{-K_r^Q(n-v)})^2 \frac{dv}{n}
\end{aligned}$$

and

$$b(n) = \left( \frac{1}{nK_r^Q} (1 - e^{-K_r^Q n}), \frac{K_r^Q}{n(K_r^Q - K_l^Q)} \left( \frac{1}{K_l^Q} (1 - e^{-K_l^Q n}) - \frac{1}{K_r^Q} (1 - e^{-K_r^Q n}) \right) \right).$$

## 2.2 Estimation Method

The conventional estimation approach for affine term-structure models is maximum likelihood (MLE) (Dai and Singleton, 2000; Duffee, 2002) or Kalman-filter-based MLE (Kim and Orphanides, 2012). Adrian et al. (2013) instead propose a three-step linear regression approach to price the time series and cross section of the term structure of interest rates, which is computationally faster and easier to implement. We apply a two-stage regression-based procedure to estimate the long-short model, motivated by the empirical estimation approach of Adrian et al. (2013). This procedure iterates between cross-sectional fitting of the yield curve to determine the  $\mathbb{Q}$ -measure parameters and time-series estimation of the factor dynamics to determine the  $\mathbb{P}$ -measure parameters.

### 2.2.1 Stage 1: Risk-Neutral Parameter Estimation

The first stage of our method estimates the parameters under the  $\mathbb{Q}$  measure and the latent state variables simultaneously by fitting the zero-coupon yields. The yields are analytical functions of the state variables  $x_t$ , allowing us to infer the unobservable latent short- and long-rate factors from the observed yields.

The time  $t$  observed yield  $Y_t = (Y_t(1), \dots, Y_t(N))'$  is a  $N \times 1$  vector where  $N$  is the number of the cross-sectional yields. We fit the yield curve by choosing  $\mathbb{Q}$  parameters  $\Theta^Q$  and state variables  $x_t$  to construct fitted yield  $y_t$

$$\min_{\Theta^Q, \{x_t\}_{t=0}^T} \sum_t (Y_t - y_t)' (Y_t - y_t).$$

Equivalently, the objective is

$$\min_{\Theta^Q} \min_{\{x_t\}_{t=0}^T} \sum_t (Y_t - y_t)'(Y_t - y_t) = \min_{\Theta^Q} \sum_t \min_{x_t} (Y_t - y_t)'(Y_t - y_t),$$

where the last equality is due to the fact that the objective is time additive. This allows us to sequentially obtain  $y_t$  and  $\Theta^Q$ . The minimization

$$\min_{x_t} (Y_t - y_t)'(Y_t - y_t)$$

is equivalent to a “cross-sectional” regression of  $Y_t$  on  $a$  and  $b$  for a given  $t$ , where  $a$  and  $b$  are calculated based on Eq.(8)

$$Y_t = a + bx_t + e_t, \tag{9}$$

where the pricing error  $e_t$  is a  $N \times 1$  vector. This yields

$$\hat{x}_t = (b'b)^{-1}b'(Y_t - a), \tag{10}$$

and is a function of  $\Theta^Q$ ,

$$\hat{x}_t = \hat{x}(\Theta^Q, Y_t).$$

The fitted error is

$$\hat{e}_t \equiv Y_t - \hat{y}_t = (Y_t - a) - b\hat{x}_t = (I - b(b'b)^{-1}b')(Y_t - a).$$

We then choose  $\Theta^Q$  to minimize the sum of squared pricing errors across all maturities and time periods

$$\min_{\Theta^Q} \sum_t \hat{e}_t' \hat{e}_t. \tag{11}$$

To obtain the optimal value of  $\Theta^Q$ , we begin by randomly selecting an initial  $\Theta^Q$  and computing the associated  $a$  and  $b$ . Given any candidate  $\Theta^Q$ , we then recover the implied time series of latent factors  $x_t$  by running the cross-sectional regression in Eq.(9). The optimal  $\Theta^Q$  is chosen to minimize the total fitted pricing error in Eq.(11). Denote this solution by  $\Theta^{Q*}$ . With the optimized risk-neutral parameters  $\Theta^{Q*}$ , we extract the time series of the latent state variables  $x_t$  by inverting the pricing equation for each time  $t$ . This is achieved via an OLS projection of the observed yields onto the estimated factor loadings in Eq.(10).

### 2.2.2 Stage 2: Physical Parameter Estimation

In the second stage, we take  $\hat{x}_t^*$  as the observed state vector, which follows the “short catch long” process under the physical measure, to estimate the physical-measure parameters  $\Theta$ . Assuming the factors follow a discrete-time approximation of a bivariate Ornstein-Uhlenbeck process, we estimate these parameters via MLE. The log-likelihood function is constructed based on the conditional distribution of  $x_{t+1}$  given  $x_t$ .

$$\Theta^* = \operatorname{argmax} - \frac{1}{2} \sum_t (\hat{x}_{t+1}^* - \mathbb{E}_t[\hat{x}_{t+1}^*]) \Sigma^{-1} (\hat{x}_{t+1}^* - \mathbb{E}_t[\hat{x}_{t+1}^*]),$$

where  $\Sigma$  is the conditional variance matrix of  $x_t$  of interval  $\Delta$ .

In theory, the volatility parameters  $\sigma_r, \sigma_l$  and their correlation  $\rho$  are invariant to the change of measure, as implied by Girsanov’s theorem. However, the empirical estimation often yields different volatility and correlation in  $\mathbb{Q}$  measure and  $\mathbb{P}$  measure. To check convergence, we compare the volatility and correlation parameters estimated in Stage 2 with the parameters in Stage 1. If the Euclidean norm of their difference is below a pre-defined tolerance threshold (e.g.,  $10^{-4}$ ), the procedure has converged. Otherwise, we return to Stage 1 and update the volatility and correlation parameters from Stage 2 as initial inputs for the next iteration. Convergence is achieved when the optimal volatility and correlation parameters in the  $\mathbb{Q}$  estimation are consistent with those estimated from the  $\mathbb{P}$  dynamics. Upon convergence, we obtain the final estimates for  $\Theta^{\mathbb{Q}^*}$  and  $\Theta^*$ .

## 2.3 Data

We estimate our long-short model using the data constructed by [Gürkaynak et al. \(2007\)](#) (GSW)<sup>2</sup>. These zero-coupon yields are based on fitted Nelson-Siegel-Svensson curves, the parameters of which are published along with the estimated zero-coupon curve. We use these parameters to back out the cross section of yields for maturities  $n = 0.25, 0.5, \dots, 10$  years, giving a cross section of  $N = 12$  maturities. We estimate all models over the sample period from January 1987 to December 2025 using daily frequency.

We supplement the yield-curve data with daily financial-market and uncertainty variables. The equity-market variable is the daily log return on the S&P 500 index, measured in percent. The dollar variable is the daily change in the U.S. dollar index (DXY), measured in basis points. We use daily changes in the VIX index, which is based on S&P 500 options, and the MOVE index, which measures Treasury-market implied volatility. The VIX, MOVE, S&P 500, and DXY series are downloaded from Bloomberg. We also use the daily

---

<sup>2</sup>We thank the authors for sharing these data for download, on the website <https://www.federalreserve.gov/econres/feds/the-us-treasury-yield-curve-1961-to-the-present.htm>.

Economic Policy Uncertainty (EPU) index of [Baker et al. \(2016\)](#), obtained from the authors' website<sup>3</sup>. Finally, we use the Treasury-market noise measure of [Hu et al. \(2013\)](#) as a proxy for market-wide Treasury illiquidity and limits to arbitrage.

For the macroeconomic analysis, we use monthly core CPI inflation and the civilian unemployment rate from FRED<sup>4</sup>. Core inflation is measured as the 12-month percentage change in the core CPI index, and unemployment is measured in percent. These variables are matched to monthly observations of Treasury constant-maturity yields and the latent factors estimated from the long-short model. For the daily inflation-expectations regressions, we use changes in the 5-year breakeven inflation rate and the 5-year, 5-year forward breakeven inflation rate from FRED.

We collect the actual monetary policy decision and the unexpected component of that decision from [Kuttner \(2001\)](#), whose dataset ends in June 2019. We also use monetary policy shocks from [Bauer and Swanson \(2022\)](#), who calculate high-frequency changes in interest rates during a 30-minute window around FOMC announcements, including 2-, 5-, and 10-year Treasury futures. Furthermore, [Bauer and Swanson \(2022\)](#) construct the monetary policy shock (MPS) by extracting the first principal component of high-frequency changes in Eurodollar futures rates (ED1 to ED4). Finally, we incorporate the target factor (surprises about the current federal funds rate target) and path factor (surprises about the expected path of the federal funds rate over the next several months) derived by [Gurkaynak et al. \(2005\)](#) to enrich our analysis.

## 2.4 Long-Short Model Estimation Results

We estimate the parameters of the long-short model using the two-stage, regression-based procedure detailed in Section 2.2. The estimation is conducted using daily zero-coupon yields from GSW for 12 maturities ranging from three months to ten years over the sample period from January 1987 to December 2025. In the first stage, the risk-neutral parameters  $\Theta^Q$  are obtained by minimizing the sum of squared pricing errors across maturities and time, and the implied state variables are extracted by projecting yields onto model-implied loadings. In the second stage, the physical parameters  $\Theta$  are estimated by maximum likelihood using the dynamics of the implied factors, and the volatility-correlation triplet  $(\sigma_r, \sigma_l, \rho)$  is updated accordingly. This procedure iterates until the estimates of volatilities and correlation converge across the  $\mathbb{Q}$  and  $\mathbb{P}$  measures.

---

<sup>3</sup><https://www.policyuncertainty.com/>

<sup>4</sup><https://fred.stlouisfed.org/>

### 2.4.1 Parameter Estimates and Economic Intuition

Table 1 presents the estimated risk-neutral and physical parameters as well as the corresponding market price of risk. The risk-neutral dynamics display moderate mean reversion, with  $K_r^Q = 0.19$  and  $K_l^Q = 0.13$ , both significant with t-statistics around 4. These values imply that, under the  $\mathbb{Q}$  measure, short rates and their long-run mean quickly adjust to shocks, ensuring well-behaved bond pricing functions. The estimated long-run risk-neutral mean  $\bar{r}^Q = 0.07$  is economically plausible and highly significant, capturing the long-run mean of the short rate in the risk-neutral world.

In contrast, the physical dynamics reveal a markedly different picture. The short-rate mean-reversion coefficient is small and insignificant ( $K_r = 0.02$ ), suggesting near-unit-root behavior of the short rate under the physical measure, with a shock half-life of more than 30 years. The long-run mean component, however, reverts more strongly ( $K_l = 0.26$ ) and is statistically significant, with a half-life of approximately 2.7 years. The physical long-run mean is estimated at  $\bar{r} = 0.05$ , which is lower than its risk-neutral counterpart. The differences between the  $\mathbb{Q}$ - and  $\mathbb{P}$ -measure parameters reveal the compensation investors require for bearing interest rate risk. For example, the risk-neutral mean reversion of the short-rate factor ( $K_r^Q = 0.19$ ) is much higher than its physical counterpart ( $K_r = 0.02$ ), implying that investors perceive short-rate shocks to be much less persistent under the risk-neutral measure than they actually are under the physical measure. Furthermore, the risk-neutral long-run mean ( $\bar{r}^Q = 0.07$ ) is considerably higher than the physical mean, contributing to a positive average term premium in bond yields. Together, these features generate a sizable and time-varying term premium, which we discuss in the next section.

The volatility estimates are tightly pinned down with  $\sigma_r = 0.01$  and  $\sigma_l = 0.03$ , with t-statistics exceeding 30. The larger value of  $\sigma_l$  underscores the importance of persistent, long-horizon shocks in shaping yield dynamics. Finally, the correlation coefficient is estimated at  $\rho = -0.05$ , with a t-statistic of -1.57, and is not statistically significant at conventional levels, suggesting that shocks to the short and long components are only weakly negatively correlated.

We further report the estimated market prices of risk, which govern the transformation from the physical to the risk-neutral dynamics and determine the compensation investors require for bearing duration risk. In the long-short model, there are two sources of duration risk. The first is the policy-driven duration risk,  $dB_t$ , which directly moves the policy-sensitive short-rate factor  $r_t$ . The second is the market-driven duration risk,  $dZ_t$ , which captures shocks to the long-run component  $l_t$  that are orthogonal to policy-driven short-rate movements. This distinction is central to the model: it allows us to separate risk compensation associated with policy-sensitive short-rate shocks from risk compensation associated

with market-driven long-rate shocks.

The most salient finding is that the priced component of duration risk comes primarily from the policy-driven shock. The estimated market price of risk associated with  $dB_t$  is large and statistically significant with  $\lambda_{br} = 21.61$ . By model construction,  $\lambda_{br} = -\lambda_{bl}$ , the market price of the  $dB_t$  shock depends on the gap between the policy-driven latent short rate and the market-driven latent long-run rate. In contrast, the estimated market prices of risk associated with the  $dZ_t$  shock are small and statistically insignificant. Thus, although the model allows for both policy-driven and market-driven duration risks, the empirically important source of priced duration risk is mostly the policy-driven component.

Since the  $dZ_t$  risk prices are statistically insignificant, the empirically relevant component of the pricing kernel can be approximated by

$$\frac{dM_t}{M_t} \simeq -r_t dt - \lambda_{br}(r_t - l_t)dB_t.$$

This expression highlights a key implication of the long-short model: the price of policy-driven duration risk is state dependent. Since the estimate of  $\lambda_{br}$  is positive, the market price of risk,  $\lambda_{br}(r_t - l_t)$ , is governed by the latent slope  $l_t - r_t$ . The relevant state variable is therefore the spread between the latent long-run rate and the latent short rate,  $l_t - r_t$ , the model-implied counterpart of the conventional yield-curve slope, often measured in the literature as the spread between the 10-year Treasury yield and the 3-month Treasury bill rate (Estrella and Mishkin, 1998; Rudebusch and Williams, 2009; Haubrich, 2021).

In normal times,  $r_t < l_t$ , the latent yield curve is upward sloping. In this region, the market price of the  $dB_t$  shock,  $\lambda_{br}(r_t - l_t)$ , is negative. A positive  $dB_t$  shock therefore raises the pricing kernel  $M_t$  and represents a bad state. At the same time, the same shock raises the short rate and lowers nominal bond prices. Long-term nominal bonds therefore pay poorly in bad states and become risky assets. Investors require a positive risk premium for holding long-duration bonds, so the term premium is high when the latent short rate is below the latent long-run rate.

By contrast, the case  $r_t > l_t$  is a special state in which the latent yield curve is inverted. In this region, the market price of the  $dB_t$  shock is positive. A negative  $dB_t$  shock raises marginal utility, lowers the short rate, and increases nominal bond prices. Long-term bonds then hedge bad states, so the required term premium is lower, all else equal. This mechanism explains why the estimated 10-year term premium loads negatively on the short-rate factor, which will be discussed later: holding the long-run component fixed, a higher  $r_t$  moves the economy closer to an inverted latent yield curve, where long-duration bonds have stronger hedging value and require less risk compensation.

Our framework therefore provides a risk-premium interpretation for why the yield-curve

slope has long been found to forecast real activity and recessions (Harvey, 1988; Estrella and Hardouvelis, 1991; Haubrich, 2021; Engstrom and Sharpe, 2019): the slope summarizes the state-dependent compensation investors require for bearing policy-driven duration risk. The conventional term spread, such as the 10-year minus 3-month spread, mixes policy-driven short-rate movements and market-driven long-rate movements. In our model, the relevant state variable is instead the latent spread  $l_t - r_t$ , which more cleanly separates the market-driven long-run component from the policy-sensitive short-rate component. Episodes with  $r_t > l_t$  are rare and typically arise when monetary policy is tight relative to the market-implied long-run rate. Historically, such episodes tend to precede NBER recessions. The most recent tightening cycle is an important exception so far: despite a sharp rise in the policy-sensitive short-rate factor and a pronounced inversion of the yield curve, it has not yet been followed by an NBER recession within our sample period.

#### 2.4.2 Model Fit

Figure 2 shows the time series of observed and fitted yields for the 3-month and 10-year Treasury yields. The long-short model tracks both ends of the curve closely across regimes, including tightening and easing monetary policy cycles. While the overall model fit is strong, during the Zero Lower Bound (ZLB) period a noticeable gap appears at the short end: the fitted 3-month yield (dashed red) remains below the observed rate (solid blue), reflecting the model’s inability to fully capture the policy-imposed floor. In contrast, the bottom panel shows that the model’s fit for the 10-year yield remains remarkably robust during the same ZLB period. This phenomenon is largely due to the simple long-short model with only two factors, which cannot capture flexible front-end curvature.

We now provide evidence on how well the long-short model fits the yield curve by investigating the time series properties of the yield pricing errors in Table 2. The average yield pricing errors are economically modest across all maturities, ranging from -2 to 2 basis points. Errors at the short end (3M, 2Y) exhibit higher volatility while those at longer maturities (5Y, 10Y) are relatively smaller.

The pricing errors across maturities are primarily due to the limited number of factors rather than the estimation method. Switching to the two-factor ACM model, estimated at the daily frequency, Panel B of Table 2 offers no significant improvement in fitting the yield curve. Its pricing errors for intermediate maturities remain elevated, and the overall error magnitudes are comparable to our model. However, when we apply the ACM model with five factors ( $K=5$ ) in Panel C, as suggested by the original study, the pricing errors shrink substantially. The mean absolute pricing error declines to just 0.3 basis points for the 3-month yield and 0.2 basis points for the 10-year yield. This pattern highlights that

the number of factors, rather than the estimation technique, is the main source of the yield curve misfit. Our goal is not to maximize in-sample fit, but to obtain an economically interpretable decomposition of the yield curve. We therefore adopt a simple yet economically meaningful arbitrage-free “short catch long” model. Finally, because yield pricing errors exhibit pronounced serial correlation and heteroskedasticity, we report Newey-West standard errors in Table 1 and results are robust to reasonable choices of bandwidth.

### 2.4.3 Latent Factors

Figure 1 plots the two latent state variables extracted from the long-short model, the short rate  $r_t$  in blue and the long-run mean  $l_t$  in red, with NBER recessions shaded. The dynamics of these factors are consistent with the parameter estimates in Table 1 and highlight the distinct roles of the short- and long-term components.

The implied short-rate  $r_t$  exhibits close alignment with monetary policy actions, rising sharply during tightening cycles (1994–95, 2004–06, 2022–24) and declining during easing episodes (2001, 2008–09, 2020). This behavior reflects its estimated near-zero mean reversion under the physical measure ( $K_r = 0.02$ ), implying that short rates follow a highly persistent, near-unit-root process. This persistence ensures that monetary policy shocks have lasting effects on the short end of the curve. In contrast, the long-run mean component  $l_t$  exhibits higher volatility than the policy-sensitive short rate and evolves gradually, with an estimated mean-reversion speed of  $K_l = 0.26$ , which corresponds to a half-life of about 2.7 years.

The two latent factors also move differently across regimes. During recessions,  $r_t$  falls quickly as the Fed eases, while  $l_t$  tends to drift upward, indicating that markets revise the long-run anchor higher relative to the contemporaneous policy stance. By contrast, in tightening episodes, especially during 2004–2006,  $r_t$  rises steeply whereas  $l_t$  trends down only gradually. This divergence echoes the well-known Greenspan conundrum: despite a 425 bp increase in the funds rate from 2004 to 2006, long-maturity yields and forward rates declined, a pattern widely attributed to a fall in the term premium associated with lower macro/market volatility and more predictable policy (Backus and Wright, 2007).

Table 3 formally investigates the relationship between  $r_t$  and  $l_t$  in a regression setting. Regressing daily changes in  $l_t$  on changes in  $r_t$  shows little relation on average, with a coefficient of -0.18 that is statistically insignificant, consistent with the weak correlation implied by the  $\rho$  parameter in Table 1. Interestingly, during tightening cycles, a rise in the policy-sensitive short-rate factor coincides with a decline in the long-run mean, which is captured by the interaction term  $\Delta r_t \times Hike$ . The point estimate for the interaction ( $-0.64$ ) indicates that a 100 bp increase in  $\Delta r_t$  is associated with a roughly 64 bp reduction in  $\Delta l_t$  during tightening cycles, whereas outside those periods the contemporaneous relationship is

near zero. The transmission from the latent short-rate factor to the latent long-rate factor is weaker during tightening cycles than during easing cycles.

## 3 Empirical Applications

### 3.1 Term Premium versus Term Spread

Yields on long-maturity bonds can be decomposed into (i) the average path of expected short-term rates over the bond’s life and (ii) a residual component, the term premium. The term premium represents the compensation investors demand for bearing the duration risk inherent in long-term bonds. Typically, expected short rates and term premia are extracted using arbitrage-free affine term-structure models, which impose cross-maturity consistency by ruling out arbitrage opportunities. [Adrian et al. \(2013\)](#) estimate such models using only yield-curve information and obtain the term-premium component. To address the small-sample bias that arises from the high persistence of interest rates, [Kim and Wright \(2011\)](#) include interest-rate survey data in the models. Other approaches incorporate macroeconomic variables alongside yield factors to capture broader sources of variation in bond yields ([Hördahl and Tristani, 2018](#)). [Cohen et al. \(2018\)](#) provide a comprehensive comparison of these frameworks, highlighting both their shared theoretical structure and key methodological differences.

While these models have advanced the understanding of yield-curve dynamics, their statistical pricing factors are less directly suited to attributing term-premium movements to economically interpretable short- and long-rate shocks. A central implication of the long-short model is that the 10-year term premium can be written as a closed-form affine function of two economically interpretable state variables: the short-rate component  $r_t$ , capturing the near-term policy rate set by the Federal Reserve, and the long-run component  $l_t$  reflecting market participants’ long-term expectations about the economy. This structure allows an analytical decomposition of yields into expected short rates and term premium, which makes it possible to explicitly evaluate how short-rate shocks affect the compensation investors demand for holding long-term bonds.

*Decompose Term Premium into Latent Factors* – We implement this decomposition of the term premium and short-rate expectations within our affine long-short model, where both components are linear in the state vector  $x_t = (r_t, l_t)'$ . A key advantage of this framework is that it explicitly maps the expectations component to the physical measure ( $\mathbb{P}$ ) and the risk compensation to the risk-neutral ( $\mathbb{Q}$ ) measure.

We write the yield on an  $n$ -year zero-coupon bond,  $y_t(n)$ , as the sum of two components: the average of expected future short rates and the term premium. The first component,

$y_t^{\text{EH}}(n)$ , is based on the Expectations Hypothesis (EH) under the physical measure ( $\mathbb{P}$ ), which represents the yield that would prevail in an economy with risk-neutral investors:

$$y_t^{\text{EH}}(n) = \frac{1}{n} \int_0^n \mathbb{E}_t^{\mathbb{P}} [r_{t+u}] du$$

The term premium,  $TP_t(n)$ , is the difference between the observed market yield and the EH yield.

$$TP_t(n) = y_t(n) - y_t^{\text{EH}}(n)$$

Within our affine framework, both components are linear functions of the state vector  $r_t$  and  $l_t$ . The observed yield is priced under the risk-neutral  $\mathbb{Q}$  measure, while the EH yield is determined by the real-world physical  $\mathbb{P}$ -measure dynamics:

$$\begin{aligned} y_t(n) &= a^{\mathbb{Q}}(n) + b^{\mathbb{Q}}(n)'x_t, \\ y_t^{\text{EH}}(n) &= a^{\mathbb{P}}(n) + b^{\mathbb{P}}(n)'x_t, \\ TP_t(n) &= (a^{\mathbb{Q}}(n) - a^{\mathbb{P}}(n)) + (b^{\mathbb{Q}}(n) - b^{\mathbb{P}}(n))'x_t \\ &= A(n) + B(n)r_t + C(n)l_t. \end{aligned} \tag{12}$$

Thus, the term premium is itself affine in  $(r_t, l_t)$ , with loadings that summarize the wedge between  $\mathbb{Q}$  and  $\mathbb{P}$  pricing. In our estimated long-short model, this permits a transparent mapping from the latent factors to the risk compensation at each maturity.

Figure 3 plots the estimated factor loadings  $b(n)$  under both  $\mathbb{Q}$  and  $\mathbb{P}$  measures. In the top panel, the short-rate loading  $b_r^{\mathbb{Q}}(n)$  decays monotonically with maturity, consistent with no-arbitrage pricing. In contrast,  $b_r^{\mathbb{P}}(n)$  decreases more gradually and lies uniformly above  $b_r^{\mathbb{Q}}(n)$ , reflecting more persistent dynamics of short rates under the physical measure. This difference arises because the mean-reversion speed of the short rate,  $K_r$ , is much smaller than its risk-neutral counterpart  $K_r^{\mathbb{Q}}$ . Economically, this implies that under the physical  $\mathbb{P}$  measure, deviations in the short rate are highly persistent, whereas under the risk-neutral  $\mathbb{Q}$  measure investors price bonds as if the short rate will revert more quickly toward its long-run mean. The wedge between these short-rate dynamics generates one source of the term premium. In the bottom panel, the loadings on the long-term component,  $b_l^{\mathbb{Q}}(n)$  and  $b_l^{\mathbb{P}}(n)$ , are both increasing and convex in maturity, with the gap widening at the long end.

Panel B of Table 1 reports the estimated decomposition of the 10-year term premium, expressed in a simple and transparent analytical form, into its constant, short-rate, and long-rate components. The constant term ( $A = 0.012$ ) is positive and statistically significant, indicating a state-independent component of the 10-year term premium. The coefficient

on the short-rate factor ( $B = -0.44$ ) is negative and statistically significant. Holding the long-rate factor fixed, a higher policy-sensitive short-rate factor is associated with a lower 10-year term premium. In contrast, the coefficient on the long-run component ( $C = 0.30$ ) is positive and significant, suggesting that increases in the long-term expectation of yields are associated with a higher term premium. Together, these results indicate that short-rate shocks and long-run expectations have offsetting effects on the term premium.

The negative loading on the short-rate factor follows from the state-dependent price of policy-driven duration risk derived in Section 2.4.1. The empirically relevant component of the pricing kernel is

$$\frac{dM_t}{M_t} \simeq -r_t dt - \lambda_{br}(r_t - l_t) dB_t,$$

with  $\lambda_{br} > 0$ , so the price of the  $dB_t$  shock is governed by  $r_t - l_t$ . When  $r_t < l_t$ , a positive  $dB_t$  shock raises marginal utility while lowering long-bond prices, so investors require compensation for bearing duration risk. Holding  $l_t$  fixed, an increase in  $r_t$  moves the economy toward a region in which long-term bonds have stronger hedging value and require less risk compensation. This mechanism maps directly into the negative estimated loading  $B = -0.44$  of the 10-year term premium on the short-rate factor.

The loading of the 10-year term premium on the latent factors is worth a closer examination. We start by plotting  $B(n)$  for the 10-year maturity as the blue line in the upper panel of Figure 4. The physical mean-reversion parameter is fixed at  $K_r^P = 0.02$ , the baseline estimate reported in Table 1, while the risk-neutral parameter  $K_r^Q$  is allowed to vary. As implied by equation (8), the factor loading  $b_r(10)$  is strictly decreasing in the mean-reversion parameter  $K_r$ . Consequently, whenever  $K_r^Q > K_r^P$ , the difference  $B(10) = b_r^Q(10) - b_r^P(10)$  becomes negative, and the magnitude of this negative loading increases as the gap between  $K_r^Q$  and  $K_r^P$  widens.

We then examine the coefficient  $C(10)$ , which is the loading of the 10-year term premium on the long-rate factor, shown as the red line in the upper panel of Figure 4. The parameters  $K_r^P = 0.02$ ,  $K_l^P = 0.26$ , and  $K_l^Q = 0.13$  are fixed at the baseline values reported in Table 1, while the risk-neutral parameter  $K_r^Q$  is allowed to vary. Whenever  $K_r^Q > K_r^P$ , the difference  $C(10) = b_l^Q(10) - b_l^P(10)$  becomes positive, and the magnitude of this positive loading increases as the gap between  $K_r^Q$  and  $K_r^P$  widens. We also consider a different specification in which the risk-neutral parameter  $K_l^Q$  is varied while holding  $K_r^P = 0.02$ ,  $K_l^P = 0.26$ , and  $K_r^Q = 0.19$  fixed. The resulting coefficient  $C(10)$  is plotted in the lower panel of Figure 4. In this case,  $C(10)$  declines monotonically with the difference  $K_l^Q - K_l^P$ .

After obtaining the factor loadings  $b(n)$ , we decompose the 10-year yield into the short-rate expectations component and the term premium in Figure 5. The top panel separates the observed yield into its EH component in blue and term premium in red using Eq. (12). The

bottom panel compares our estimated 10-year term premium with that from the five-factor ACM model using daily zero-coupon yields<sup>5</sup>. The two series track each other closely, with remarkably similar trends and dynamics. Despite slight differences in level, both estimates capture major peaks and troughs around economic turning points.

*Decompose Term Premium into Sources of Risk* – We next examine the sources of the term premium by providing another decomposition of the 10-year term premium. The model contains two sources of duration risk: the policy-driven duration shock  $dB_t$ , which directly moves the policy-sensitive short-rate factor  $r_t$ , and the market-driven duration shock  $dZ_t$ , which captures orthogonal movements in the long-run component  $l_t$ . We therefore decompose the 10-year term premium into the compensation for bearing  $dB_t$  risk and the residual compensation for bearing  $dZ_t$  risk. This decomposition is implemented through counterfactual pricing exercises that shut down one Brownian risk price at a time and compare the resulting risk-neutral yield with the physical-measure expectations component.

Figure 6 reports the result. The black line plots the full 10-year term premium, the blue area shows the contribution from the policy-driven  $dB_t$  risk, and the red area shows the residual contribution from the market-driven  $dZ_t$  risk. Consistent with the market-price-of-risk estimates in Section 2.4.1, most of the 10-year term premium represents compensation for the policy-driven duration shock. Using the daily counterfactual series from 1987 to 2025, the policy-driven  $dB_t$  component accounts for 76.7% of its time-series variation. The contribution from  $dZ_t$  risk is comparatively small. Thus, although the model allows for both policy-driven and market-driven sources of duration risk, the empirically important component of risk compensation is the policy-driven one.

This decomposition highlights a key contribution of the long–short model relative to the five-factor ACM model of Adrian et al. (2013). The ACM model provides a flexible estimate of the time-varying term premium using five principal components of yields as pricing factors. Consistent with this benchmark, our estimated 10-year term premium closely tracks the ACM term premium and captures similar peaks and troughs around economic turning points. However, because ACM factors are statistical yield-curve factors, the resulting term premium is harder to map into economically interpretable sources of risk. In contrast, the long–short model links the term premium directly to two model-implied sources of duration risk: the policy-driven  $dB_t$  shock and the market-driven  $dZ_t$  shock. The decomposition in Figure 6 therefore shows not only the magnitude of the term premium, but also what type of risk it primarily compensates. The evidence indicates that the policy-sensitive shock is the dominant source of 10-year term-premium variation.

---

<sup>5</sup>In the original paper, ACM first apply the five-factor ACM model to monthly data and then use the estimated parameters to back out the daily term premium. In our paper, we apply their model directly to the daily data to obtain the daily term premium.

Figure 6 also highlights the close connection between the 10-year term premium and the latent term spread  $l_t - r_t$ , shown by the dashed gray line. The correlation between the two series is as high as 0.96. This strong co-movement is consistent with the risk-pricing mechanism of the long-short model. In the stochastic discount factor, the price of the policy-driven duration shock is proportional to  $r_t - l_t$ , implying that risk compensation varies with the latent slope of the yield curve. When  $l_t - r_t$  is high, the policy-sensitive short rate is low relative to the market-implied long-run component. In this region, long-duration Treasuries are more exposed to policy-driven duration risk, and investors require a higher term premium for holding them.

Conversely, when  $l_t - r_t$  narrows or turns negative, the policy-sensitive short rate is high relative to the long-run component. Long-duration bonds then have stronger hedging value, and the required compensation for bearing duration risk declines. The figure therefore shows that the latent spread  $l_t - r_t$  is not merely a measure of the yield-curve slope; it also summarizes the state-dependent risk compensation embedded in long-term Treasury yields.

*Countercyclical Pattern* – The estimated term premium exhibits a pronounced countercyclical pattern, which aligns with the notion that it serves as a risk premium for holding long-term bonds in the face of macroeconomic volatility. During economic expansions or tightening cycles, increases in the 10-year yield are largely driven by the expectations component, while the premium remains stable or even declines. In contrast, during periods of macroeconomic stress, such as the 2008 Global Financial Crisis (GFC) or COVID-19 shock, the term premium rises, reflecting heightened risk aversion. After the GFC, the term premium shows a persistent downward trend, consistent with a broader secular decline in risk compensation documented in the literature (Cohen et al., 2018). This decline reflects a combination of structural forces, including reduced macroeconomic volatility, enhanced central bank credibility, and increased demand for long-term safe assets from institutional investors. In related evidence, Bauer and Chernov (2024) show that a risk measure based on the conditional skewness of Treasury yields increases as the Fed lowers the policy rate and falls during tightening cycles.

This countercyclical behavior naturally induces a negative co-movement between the EH component and the term premium. As shown in Figure 5, periods of rising expected short rates (e.g., recoveries or policy tightening) are typically associated with flat or declining term premia. Rising rate expectations in such periods are often interpreted as signals of macroeconomic strength and future growth, which compress required risk compensation. Conversely, when uncertainty rises and the outlook deteriorates, expected short rates fall sharply, but investors demand a higher premium to bear risk in the face of elevated uncertainty, causing the term premium to rise.

We further explore the negative relationship between the short-rate expectations compo-

ment and the term premium using the decompositions from [Kim and Orphanides \(2012\)](#) and [Adrian et al. \(2013\)](#) in [Figure 7](#). The correlation between 1-year short-rate expectations and the 10-year term premium in the long-short model is around -0.43, and in the ACM model it is around -0.31. However, the correlation in the KW model is positive at around 0.55.

The difference with the KW model likely reflects the role of survey information, displayed in panel D of [Figure 7](#), in disciplining expected short rates. As shown by [Cieslak \(2018\)](#), professional forecasters and investors tend to overestimate future short rates during recessions and underestimate them during recoveries, producing large and persistent expectational errors over the business cycle. These forecast errors lead survey-based measures of expected short rates to move in the same direction as realized term premium.

For any given yield, the term premium is measured as the residual after subtracting the estimated expectations component. This residual construction implies that any bias in the estimated expectations component is mechanically reflected with the opposite sign in the inferred term premium. If expected short rates are estimated too high, the residual term premium is estimated too low; if expected short rates are estimated too low, the residual term premium is estimated too high.

This mechanical link becomes important when survey forecasts contain systematic business-cycle errors. As shown by [Cieslak \(2018\)](#), professional forecasters tend to overpredict future short rates in recessions and underpredict them in recoveries. A survey-disciplined term-structure model can therefore inherit these forecast errors. During recessions, survey forecasts may not fall enough relative to the true expected path of short rates, leading the model to attribute too much of the yield to expectations and too little to the term premium. During recoveries, survey forecasts may rise too slowly, leading the model to understate the expectations component and overstate the residual term premium. These cyclical forecast errors can distort the implied comovement between expected short rates and term premia.<sup>6</sup>

In contrast, data-driven decompositions such as those in ACM and our long-short model infer expectations directly from the cross section of yields, abstracting from survey information. A possible explanation for the difference with KW is that survey information embeds cyclical forecast errors, which can alter the residual term-premium component in survey-disciplined decompositions. This distinction helps explain why the long-short and ACM

---

<sup>6</sup>A simple example illustrates the point. Suppose that in normal times the two-year yield is 8%, consisting of a 4% expectations component and a 4% term premium. Entering a recession, the two-year yield falls to 6%. If survey forecasters expect short rates to remain relatively high, the survey-implied expectations component may be 3%. The residual term premium is then also 3%, so both the estimated expectations component and the estimated term premium decline from 4% to 3%. However, if the true expected path of short rates is closer to 1% because the Fed cuts more aggressively than forecasters anticipate, the true residual term premium is 5%. In this case, the survey-based decomposition incorrectly makes the expectations component and the term premium appear to move together, whereas the true decomposition implies that expected short rates fall and the term premium rises.

models yield a negative correlation between expected short rates and term premia, consistent with the countercyclical nature of risk compensation, whereas the KW model shows the opposite pattern.

### 3.2 The Response of Long-term Rates to Monetary Policy

We now apply our long-short model to a key setting for identifying monetary policy surprises: Federal Open Market Committee (FOMC) announcements. Since [Kuttner \(2001\)](#), a large literature has examined how financial markets respond to unexpected changes in short-term interest rates around these announcements. While monetary policy shocks affect a range of asset classes, including equities, exchange rates, and sovereign debt, their transmission to the long end of the yield curve remains a central question in macroeconomics and finance. Understanding this transmission is critical, as long-term yields directly shape domestic financial conditions, borrowing costs, and savings returns, and thereby the effects on real activity.

Two competing views about how monetary policy shocks affect long-term interest rates exist. The first emphasizes that a tightening (easing) shock should lead to a significant rise (decline) in long-term yields. This view is formalized in models such as [Jansen et al. \(2024\)](#) and [Kekre et al. \(2024\)](#), which show that short-term rates influence long-term yields not only through expectations but also through the term premium. In these models, arbitrageurs play a critical role: when the Fed adopts tightening monetary policy, investors shift toward shorter maturities, forcing arbitrageurs to absorb more duration risk, which increases the term premium and amplifies the rise in long-term yields. There is accumulating empirical evidence supporting the mechanism that tightening monetary policy raises long rates by more than changes in expected short rates can explain ([Gertler and Karadi, 2015](#); [Gilchrist et al., 2015](#); [Hanson and Stein, 2015](#); [Hanson et al., 2021](#)).

In contrast, the second theoretical camp suggests that long-term rates underreact to monetary policy shocks. This view is rooted in dynamic preferred-habitat models such as [Vayanos and Vila \(2021\)](#), where risk-averse arbitrageurs and maturity-specific bond demand jointly determine bond prices. Risk-averse arbitrageurs transmit shocks from the short-term interest rate to long-term rates through carry trades. For example, when the central bank lowers the short-term interest rate, arbitrageurs find it profitable to borrow at the short rate and buy longer-term bonds, which lowers long-term yields. However, because these arbitrageurs are not risk neutral, they limit their trades to manage interest-rate risk, which causes long-term rates to underreact to policy shocks.

Our paper contributes to this debate by taking a step back and considering a simple and transparent arbitrage-free affine term-structure benchmark. In our long-short model,

we back out the implied short rate  $r_t$  and the long-run mean  $l_t$  from the cross section of zero-coupon yields. Unlike prior studies that rely on observed 10-year yields (Gertler and Karadi, 2015; Gilchrist et al., 2015) or forward rates (Hanson and Stein, 2015), both of which mix implied short-rate and long-rate components, our model allows us to separately identify these effects cleanly. This decomposition allows us to assess the transmission of monetary policy shocks to the short and long ends of the yield curve with greater precision.

Monetary policy surprises are typically identified using intraday changes in money-market futures rates within a narrow window surrounding FOMC announcements. Following the literature, we adopt several monetary surprises: (1) the surprise component from Kuttner (2001), which measures unanticipated changes in current-month federal funds futures; (2) the individual ED1–ED4 (Eurodollar) futures surprises to trace the maturity-specific (one- to four-quarter) sensitivity of the yield curve (Bauer and Swanson, 2022); and (3) the target and path factors from Gurkaynak et al. (2005), which separately identify surprises to the contemporaneous federal funds target and forward guidance from the Fed regarding the future policy path. To assess the transmission of monetary policy shocks along the yield curve, we regress changes in our model-implied short-term rate  $r_t$  and long-run mean  $l_t$  on these high-frequency monetary surprises, using only observations on FOMC announcement days.

Table 4 shows that the implied short-term yield on FOMC announcement days responds strongly to monetary policy surprises across all specifications. A 100-basis-point increase in the current-quarter Eurodollar futures surprise (ED1) around the tight FOMC announcement window is associated with a 63-basis-point increase in the implied short-term yield estimated from our long-short model. Interestingly, we observe a hump-shaped pattern in the magnitude of the response across Eurodollar maturities. The impact of monetary surprises increases from the Kuttner surprise to ED2, with ED2 exhibiting the largest coefficient, suggesting that market participants revise their expectations of short rates most sharply over the one-to-two-quarter horizon following the FOMC announcement. The response then tapers off at longer maturities (ED3 and ED4), indicating more muted revisions to 6- to 12-month-ahead rate expectations. Moreover, both the target and path factors from Gurkaynak et al. (2005) significantly affect the short-rate component, reinforcing that our model-implied short end is tightly linked to high-frequency policy news.

However, the response of the long-term component  $l_t$  is much weaker and depends on the shock measure. The market-based Eurodollar surprises (ED1–ED4) and the GSS target and path factors have small and statistically insignificant effects on  $l_t$ . The Kuttner current-month surprise and the raw Fed decision are negatively associated with  $l_t$  on FOMC announcement days. Thus, the strongest evidence for limited long-rate transmission comes from the futures-based and GSS measures, where monetary policy surprises mainly move

the short-rate component and have little effect on the implied long-term component in our frictionless, arbitrage-free term-structure model.

Our estimates show that market-based monetary policy surprises induce significant movements in the implied short-rate component  $r_t$ , but leave the long-run component  $l_t$  statistically unchanged. This contrasts with previous literature that argues long-term yields overreact to monetary policy shocks (Hanson and Stein, 2015; Hanson et al., 2021). A key distinction lies in the identification of policy shocks. Those earlier studies typically proxy monetary policy shocks using changes in 1-year or 2-year Treasury yields on the announcement day<sup>7</sup>, implicitly assuming these yields reflect pure expectations about future short rates.

However, short-term yields such as the 1-year rate contain both expectations and term-premium components, and the latter can be highly volatile at high frequencies (Moench and Soofi-Siavash, 2022). As a result, when long-term yields are regressed on shorter-term yields, contemporaneous movements in the term premium across maturities can mechanically inflate the estimated sensitivity, especially at high frequencies (e.g., daily), where the variance ratio of the 1-year term premium in the 1-year yield is highest. Put differently, regressing long-term yields on 1-year yield changes may introduce an “excess sensitivity” to monetary policy because of a shared term-premium channel rather than a positive response of long-term term premia to monetary policy surprises.

By contrast, our identification strategy relies on intraday changes in money-market futures within a narrow FOMC window, which isolate monetary shocks originating from very short maturities. Moreover, our dependent variable is the model-implied long-run yield component  $l_t$ , which by construction abstracts from short-term fluctuations in  $r_t$ . Together, these features allow us to cleanly separate the transmission of monetary policy to different segments of the yield curve. By leveraging arbitrage-free yield decompositions and high-frequency surprise measures with clean identification, our results provide a complementary and more nuanced picture of how monetary policy shocks propagate along the yield curve.

### 3.3 Market and Macroeconomic Drivers of Short and Long Rates

The previous applications use the long-short model to separate components that are otherwise mixed in observed yields. First, the term-premium decomposition shows that risk compensation loads differently on the policy-sensitive short-rate factor  $r_t$  and the market-driven long-rate component  $l_t$ . Second, the monetary-policy evidence shows that high-frequency

---

<sup>7</sup>Hanson and Stein (2015) further perform a robustness check and use intraday change in two-year yields in a narrow 60-minute window around each FOMC announcement as an instrument for the two-day change in two-year yields. The coefficient from regressing nominal forwards on the instrument is no longer significant, while the coefficient for real forwards remains significant.

policy surprises primarily move  $r_t$ , while leaving  $l_t$  largely unaffected. In this section, we take a broader view and ask what drives these two latent components outside monetary-policy event windows. Specifically, we examine whether financial-market conditions and macroeconomic fundamentals load differently on  $r_t$  and  $l_t$ .

This exercise helps clarify the economic drivers of the two latent factors. If  $r_t$  captures the policy-sensitive short end of the curve, it should be closely related to variables that summarize near-term policy expectations, funding conditions, and short-rate movements. If  $l_t$  captures the market-driven long-rate component, it should comove with broader financial-market conditions, uncertainty, and macroeconomic fundamentals. This exercise also illustrates why observed yields, including the observed 10-year yield, are imperfect proxies for the latent components. Since the 10-year yield is an affine combination of both  $r_t$  and  $l_t$ , regressions using observed long-maturity yields can confound policy-driven short-rate movements with market-driven long-rate movements.

Table 5 reports daily regressions of financial-market variables on interest-rate changes. Panel A uses daily changes in the latent long- and short-rate factors. Panel B uses daily changes in the 10-year and 3-month Treasury constant-maturity yields.

For the stock market, both latent factors are positively and significantly correlated with the S&P 500 return. This relation is consistent with a risk-on/risk-off view of the joint movement between equity and Treasury markets. During risk-off episodes, equity prices fall, investors rebalance toward safe and liquid Treasury securities, and the resulting flight-to-safety demand pushes Treasury prices up and yields down. During risk-on episodes, equity prices rise, safe-asset demand weakens, and Treasury yields tend to increase. The positive coefficients therefore capture the positive comovement between equity returns and yield changes.

A similar case appears for the U.S. dollar index. Both latent factors are positively and significantly related to dollar movements, but the loading on the short-rate factor is much larger than that on the long-rate factor. This pattern is consistent with the standard interest-rate-differential channel in exchange rates: a stronger dollar is closely associated with news about higher U.S. short rates and tighter expected monetary policy, which increases the relative attractiveness of dollar-denominated assets.

Without the long-short decomposition, this interpretation would be obscured. In Panel B, both constant-maturity yields are positively and significantly related to dollar movements, but the coefficient on the 10-year yield is larger than that on the 3-month yield (0.68 versus 0.30). This differs from Panel A, where the latent short-rate factor clearly dominates the latent long-rate factor. Thus, constant-maturity yields recover part of the short-rate relation, but observed yields still do not cleanly separate policy-sensitive short-rate news from market-driven long-rate movements.

The volatility measures further highlight the distinction between equity-market fear and bond-market uncertainty. VIX and MOVE are often highly correlated and are frequently used as broad measures of market uncertainty. Yet they load very differently on the latent long-rate component. In Panel A, increases in the long-rate component are associated with a significant decline in VIX but a significant increase in MOVE. The negative VIX coefficient is consistent with a standard risk-on/risk-off view of Treasury markets. In risk-off episodes, VIX rises as equity-market uncertainty increases, and investors move into safe and liquid Treasury securities. The resulting flight-to-safety demand raises Treasury prices and lowers yields. In risk-on episodes, VIX falls, safe-asset demand weakens, and long rates tend to rise. This mechanism generates a negative relation between VIX and the long-rate component.

By contrast, the positive MOVE coefficient indicates that the long-rate component is closely connected to bond-market uncertainty. Unlike VIX, which captures equity-market fear and is associated with flight-to-safety declines in yields, MOVE captures uncertainty directly in the Treasury market. This difference is visible in the opposite signs: VIX is high when flight-to-safety demand pushes long rates down, whereas MOVE is positively related to the market-driven long-rate component. The orthogonalized MOVE column,  $\text{MOVE}^\perp$ , removes the component of MOVE that is linearly explained by VIX and delivers an even cleaner version of this result: latent long-rate changes have a positive and significant coefficient, while short-rate changes are essentially unrelated. The EPU index displays a similar pattern: policy uncertainty is positively and significantly related to long-rate changes, but has little relation with short-rate changes. Together, the MOVE and EPU results suggest that  $l_t$  is especially sensitive to uncertainty that matters for long-duration Treasury pricing, including bond-market volatility and uncertainty about the policy environment.

The Treasury-market noise measure of [Hu et al. \(2013\)](#) provides a complementary perspective on the liquidity dimension of the yield curve. This measure captures deviations of individual Treasury prices from a smooth fitted yield curve and is commonly interpreted as a market-wide proxy for Treasury-market illiquidity and limits to arbitrage. In contrast to MOVE and EPU, which are mainly associated with the market-driven long-rate component, the noise measure is primarily related to the policy-sensitive short-rate factor. Panel A shows that the short-rate coefficient is negative and highly significant, whereas the long-rate coefficient is small and statistically insignificant. This pattern suggests that Treasury-market noise is more closely connected to short-rate and funding conditions than to long-rate movements. When  $r_t$  falls, particularly in stress episodes in which monetary policy eases and arbitrage capital becomes constrained, Treasury-market noise tends to increase. Conversely, increases in  $r_t$  are associated with lower noise and more orderly Treasury pricing.

We next turn from financial markets to inflation and labor-market conditions. [Table 6](#) reports two sets of regressions. Panel A uses monthly data and regresses the observed 3-month

and 10-year Treasury constant-maturity yields and the two latent factors on year-over-year core CPI inflation and the unemployment rate. These two macro variables map naturally into the Federal Reserve’s dual mandate: price stability and maximum employment. Core inflation loads positively and significantly on all four interest-rate measures. A one percentage point increase in core CPI inflation is associated with a 1.06 percentage point higher 3-month constant-maturity yield, a 0.98 percentage point higher 10-year constant-maturity yield, a 1.08 percentage point higher latent short rate, and a 1.31 percentage point higher latent long rate. This broad positive relation is consistent with inflation raising both near-term policy-rate expectations and the long-run nominal-rate anchor.

Panel B uses daily changes in market-based inflation expectations. The dependent variables are daily changes in the 3-month and 10-year Treasury constant-maturity yields and in  $r_t$  and  $l_t$ . The explanatory variables are daily changes in the 5-year breakeven inflation rate and the 5-year, 5-year forward breakeven inflation rate. Both measures are most strongly related to the latent long-rate component. A one percentage point increase in the 5-year breakeven inflation rate is associated with a 1.03 percentage point increase in  $l_t$ , compared with a 0.09 percentage point increase in  $r_t$ . The 5-year, 5-year forward breakeven inflation rate shows a similar pattern: its coefficient is 1.05 for  $l_t$ , while the coefficient for  $r_t$  is small and statistically insignificant. The observed 10-year constant-maturity yield also responds much more strongly than the 3-month constant-maturity yield. Thus, daily repricing of market-based inflation expectations is concentrated at the long end of the curve and is captured more cleanly by  $l_t$  than by the policy-sensitive short-rate factor.

The unemployment rate reveals a sharper distinction between the policy-sensitive short rate and the market-driven long rate. Its coefficient is negative and highly significant for the 3-month constant-maturity yield and for  $r_t$ : a one percentage point increase in unemployment is associated with a 37 basis point decline in the 3-month constant-maturity yield and a 44 basis point decline in the latent short-rate factor. This is exactly what one would expect from the monetary policy reaction function: when labor-market slack rises, the Federal Reserve tends to ease, pushing down the short end of the yield curve.

By contrast, the unemployment rate is positively and significantly related to  $l_t$ . A one percentage point increase in unemployment is associated with an 81 basis point increase in the latent long-rate component. Importantly, this relation is completely obscured when one uses the observed 10-year constant-maturity yield: the coefficient of unemployment on  $CMT_t^{(10)}$  is small and statistically insignificant. The reason is that the observed 10-year constant-maturity yield combines two opposing forces. Higher unemployment lowers the policy-sensitive short-rate component through expected monetary easing, but it is associated with a higher market-driven long-rate component, reflecting the long-run pricing of macroeconomic risk and uncertainty. These two forces offset each other in the observed

10-year constant-maturity yield, making the reduced-form relation appear weak.

Figure 8 visualizes this point directly. The scatter plot of the unemployment rate against  $l_t$  shows a clear positive relation, whereas the same plot using the observed 10-year constant-maturity yield is much flatter. This figure provides a simple graphical summary of the main message in Table 6: the long-short decomposition uncovers a strong relation between labor-market conditions and the market-driven long rate that is hidden in observed long-maturity yields.

Taken together, the empirical results show that the latent long-rate component is not merely a relabeling of the observed 10-year constant-maturity yield. It has distinct economic content. Financial-market uncertainty, especially bond-market volatility and policy uncertainty, loads strongly on  $l_t$ . Macro fundamentals and market-based inflation expectations also load differently on  $r_t$  and  $l_t$ : inflation raises both components, unemployment lowers the short-rate factor but raises the long-rate factor, and daily breakeven inflation changes are most closely associated with  $l_t$ . These findings reinforce the central premise of the long-short model. Observed long-term yields mix policy-driven short-rate movements with market-driven long-rate movements; separating the two components reveals economic relationships that are otherwise hidden in reduced-form yield regressions.

## 4 Conclusions

This paper develops a simple and transparent arbitrage-free affine term-structure model that separates the policy-sensitive short-rate component from the market-driven long-rate component of U.S. Treasury yields. The key economic structure is that the short rate mean-reverts toward a time-varying long-run component, which we call the “short catch long” mechanism. This specification preserves the tractability of affine term-structure models while giving the two latent factors direct economic interpretations. It also delivers closed-form expressions for bond yields, expected short-rate components, and term premia.

Estimating the model from the cross section of U.S. zero-coupon Treasury yields, we find that the two latent factors capture distinct forces in the yield curve. The extracted short-rate factor closely tracks the observed 3-month yield and moves with monetary policy cycles. The extracted long-rate factor, by contrast, differs sharply from the observed 10-year yield. This distinction is central to the paper: observed long-maturity yields are not clean measures of long-run rates, because they combine policy-sensitive short-rate movements, market-driven long-rate movements, and time-varying risk compensation.

The model gives a direct economic interpretation to term-premium variation. The 10-year term premium can be written as  $TP_t(10) = A + Br_t + Cl_t$ , with a significantly negative

loading on  $r_t$  and a significantly positive loading on  $l_t$ . The estimated term premium closely tracks the ACM benchmark, but the long-short model further attributes its movements to economically interpretable shocks. The decomposition shows that the policy-sensitive shock is the dominant source of 10-year term-premium variation, while the market-driven shock plays a smaller role. Empirically, the term premium is countercyclical: it rises during periods of macroeconomic stress and monetary easing, and tends to compress during expansions and tightening cycles. This pattern generates a negative relation between expected short rates and term premia, consistent with the ACM decomposition.

The monetary-policy evidence reinforces the importance of separating the two components. High-frequency surprises around FOMC announcements move the latent short-rate factor strongly and significantly. The long-rate component, however, shows little systematic response to the market-based Eurodollar surprises and the Gurkaynak–Sack–Swanson target and path factors. These results suggest that monetary policy announcements mainly revise near-term policy-rate expectations, rather than the market-driven long-run component of the yield curve. They also caution against treating 1-year or 2-year Treasury yields as pure measures of policy news, since those yields can contain high-frequency term-premium variation.

Finally, the market and macroeconomic regressions show that the latent long-rate component is not merely a relabeling of the observed 10-year yield. Equity returns and the U.S. dollar are related to both latent factors, with especially strong loadings on the short-rate factor. Constant-maturity yields recover part of these relations, but they still do not cleanly separate policy-sensitive short-rate news from market-driven long-rate movements. Uncertainty variables sharpen the distinction: VIX is negatively related to the long-rate component through flight-to-safety episodes, while MOVE, orthogonalized MOVE, and policy uncertainty are positively related to it. Treasury-market noise is instead tied primarily to the short-rate factor, pointing to a liquidity and funding dimension that is hidden in observed yields. At the monthly frequency, inflation raises both latent components, whereas unemployment lowers the short-rate factor but raises the long-rate factor, a relation that is obscured in the observed 10-year yield.

Taken together, our results show that the long-short framework provides a transparent benchmark for studying term premia, monetary transmission, and the macro-financial drivers of long-term yields. By separating policy-driven short-rate movements from market-driven long-rate movements, the model reveals economic relationships that are otherwise hidden in reduced-form regressions using observed Treasury yields.

## References

- Adrian, T., R. K. Crump, and E. Moench (2013). Pricing the term structure with linear regressions. *Journal of Financial Economics* 110(1), 110–138.
- Ang, A. and M. Piazzesi (2003). A no-arbitrage vector autoregression of term structure dynamics with macroeconomic and latent variables. *Journal of Monetary Economics* 50(4), 745–787.
- Backus, D. and J. H. Wright (2007). Cracking the conundrum.
- Baker, S. R., N. Bloom, and S. J. Davis (2016). Measuring economic policy uncertainty. *The Quarterly Journal of Economics* 131(4), 1593–1636.
- Bauer, M. and M. Chernov (2024). Interest rate skewness and biased beliefs. *The Journal of Finance* 79(1), 173–217.
- Bauer, M. D. and E. T. Swanson (2022). A reassessment of monetary policy surprises and high-frequency identification. Technical report, National Bureau of Economic Research.
- Bekaert, G., E. Engstrom, and A. Ermolov (2021). Macro risks and the term structure of interest rates. *Journal of Financial Economics* 141(2), 479–504.
- Bianchi, F., M. Lettau, and S. C. Ludvigson (2022). Monetary policy and asset valuation. *The Journal of Finance* 77(2), 967–1017.
- Bok, B., T. M. Mertens, and J. C. Williams (2025). Macroeconomic drivers and the pricing of uncertainty, inflation, and bonds. *Journal of Financial Economics* 172, 104130.
- Campbell, J. Y., C. Pflueger, and L. M. Viceira (2020). Macroeconomic drivers of bond and equity risks. *Journal of Political Economy* 128(8), 3148–3185.
- Chen, R.-R. and L. Scott (1992). Pricing interest rate options in a two-factor cox–ingersoll–ross model of the term structure. *The Review of Financial Studies* 5(4), 613–636.
- Christensen, J. H., F. X. Diebold, and G. D. Rudebusch (2011). The affine arbitrage-free class of nelson–siegel term structure models. *Journal of Econometrics* 164(1), 4–20.
- Cieslak, A. (2018). Short-rate expectations and unexpected returns in treasury bonds. *The Review of Financial Studies* 31(9), 3265–3306.
- Cieslak, A. and P. Povala (2016). Information in the term structure of yield curve volatility. *The Journal of Finance* 71(3), 1393–1436.

- Cohen, B. H., P. Hördahl, and F. D. Xia (2018). Term premia: models and some stylised facts. *BIS Quarterly Review September*.
- Cox, J. C., J. E. Ingersoll, S. A. Ross, et al. (1985). A theory of the term structure of interest rates. *Econometrica* 53(2), 385–407.
- Dai, Q. and K. J. Singleton (2000). Specification analysis of affine term structure models. *The Journal of Finance* 55(5), 1943–1978.
- Duffee, G. R. (2002). Term premia and interest rate forecasts in affine models. *The Journal of Finance* 57(1), 405–443.
- Duffie, D. and R. Kan (1996). A yield-factor model of interest rates. *Mathematical Finance* 6(4), 379–406.
- Engstrom, E. C. and S. A. Sharpe (2019). The near-term forward yield spread as a leading indicator: A less distorted mirror. *Financial Analysts Journal* 75(4), 37–49.
- Estrella, A. and G. A. Hardouvelis (1991). The term structure as a predictor of real economic activity. *The Journal of Finance* 46(2), 555–576.
- Estrella, A. and F. S. Mishkin (1998). Predicting U.S. recessions: Financial variables as leading indicators. *Review of Economics and Statistics* 80(1), 45–61.
- Gertler, M. and P. Karadi (2015). Monetary policy surprises, credit costs, and economic activity. *American Economic Journal: Macroeconomics* 7(1), 44–76.
- Gilchrist, S., D. López-Salido, and E. Zakrajšek (2015). Monetary policy and real borrowing costs at the zero lower bound. *American Economic Journal: Macroeconomics* 7(1), 77–109.
- Gurkaynak, R., B. Sack, and E. Swanson (2005). Do actions speak louder than words? the response of asset prices to monetary policy actions and statements. *International Journal of Central Banking* 1(1), 55–93.
- Gürkaynak, R. S., B. Sack, and J. H. Wright (2007). The US treasury yield curve: 1961 to the present. *Journal of Monetary Economics* 54(8), 2291–2304.
- Hanson, S. G., D. O. Lucca, and J. H. Wright (2021). Rate-amplifying demand and the excess sensitivity of long-term rates. *The Quarterly Journal of Economics* 136(3), 1719–1781.
- Hanson, S. G. and J. C. Stein (2015). Monetary policy and long-term real rates. *Journal of Financial Economics* 115(3), 429–448.

- Harvey, C. R. (1988). The real term structure and consumption growth. *Journal of Financial Economics* 22(2), 305–333.
- Haubrich, J. G. (2021). Does the yield curve predict output? *Annual Review of Financial Economics* 13, 341–362.
- Hördahl, P. and O. Tristani (2018). Inflation risk premia in the euro area and the united states. *36th issue (September 2014) of the International Journal of Central Banking*.
- Hu, G. X., J. Pan, and J. Wang (2013). Noise as information for illiquidity. *The Journal of Finance* 68(6), 2341–2382.
- Jansen, K. A., W. Li, and L. Schmid (2024). Granular treasury demand with arbitrageurs. Technical report, National Bureau of Economic Research.
- Joslin, S., K. J. Singleton, and H. Zhu (2011). A new perspective on gaussian dynamic term structure models. *The Review of Financial Studies* 24(3), 926–970.
- Kekre, R., M. Lenel, and F. Mainardi (2024). Monetary policy, segmentation, and the term structure. Technical report, National Bureau of Economic Research.
- Kim, D. H. and A. Orphanides (2007). The bond market term premium: what is it, and how can we measure it? *BIS Quarterly Review*, June.
- Kim, D. H. and A. Orphanides (2012). Term structure estimation with survey data on interest rate forecasts. *Journal of Financial and Quantitative Analysis* 47(1), 241–272.
- Kim, D. H. and J. H. Wright (2011). An arbitrage-free three-factor term structure model and the recent behavior of long-term yields and distant-horizon forward rates.
- Kuttner, K. N. (2001). Monetary policy surprises and interest rates: Evidence from the Fed funds futures market. *Journal of Monetary Economics* 47(3), 523–544.
- Moench, E. and S. Soofi-Siavash (2022). What moves treasury yields? *Journal of Financial Economics* 146(3), 1016–1043.
- Pflueger, C. (2025). Back to the 1980s or not? the drivers of inflation and real risks in Treasury bonds. *Journal of Financial Economics* 167, 104027.
- Rudebusch, G. D. and J. C. Williams (2009). Forecasting recessions: The puzzle of the enduring power of the yield curve. *Journal of Business & Economic Statistics* 27(4), 492–503.

Vasicek, O. (1977). An equilibrium characterization of the term structure. *Journal of Financial Economics* 5(2), 177–188.

Vayanos, D. and J.-L. Vila (2021). A preferred-habitat model of the term structure of interest rates. *Econometrica* 89(1), 77–112.

**Table 1: Estimates of the Long-Short Model**

Panel A: Risk-Neutral and Physical Parameters			
Parameter	Estimate	Std. Error	T-Statistic
$K_r^Q$	0.19	0.04	4.50
$K_l^Q$	0.13	0.03	4.07
$\bar{r}^Q$	0.07	0.00	51.90
$K_r$	0.02	0.03	0.79
$K_l$	0.26	0.11	2.33
$\bar{r}$	0.05	0.02	3.03
$\sigma_r$	0.01	0.00	32.10
$\sigma_l$	0.03	0.00	70.91
$\rho$	-0.05	0.03	-1.57
$\lambda_{br}$	21.61	3.69	5.86
$\lambda_{zr}$	1.07	0.67	1.60
$\lambda_{zl}$	-5.84	4.12	-1.42
$\lambda_{z0}$	0.17	0.29	0.57
Panel B: 10Y Term Premium Decomposition			
Coefficient	Estimate	Std. Error	T-Statistic
A	0.012	0.00	2.74
B	-0.44	0.14	-3.25
C	0.30	0.09	3.20

This table summarizes the estimates of risk-neutral and physical parameters for the long-short model using two-stage regression-based procedure in Panel A. Panel B reports the model estimation of  $TP_t(n) = A + Br_t + Cl_t$ . Standard errors are computed using a GMM framework with a Heteroskedasticity and Autocorrelation Consistent (HAC) covariance matrix estimator (Newey-West). The sample period is from January 1987 to December 2025.

**Table 2: Model Fit Diagnostics**

	Panel A: Yield Pricing Errors from Long-Short Model					Panel B: Yield Pricing Errors from ACM (K=2)					Panel C: Yield Pricing Errors from ACM (K=5)				
	n=0.25	n=2	n=5	n=10		n=0.25	n=2	n=5	n=10		n=0.25	n=2	n=5	n=10	
mean	0.02	-0.02	0.01	-0.02		0.01	0.06	0.09	-0.01	mean	0.003	-0.002	-0.003	-0.002	
std	0.20	0.15	0.09	0.14		0.32	0.19	0.12	0.12	std	0.02	0.00	0.00	0.01	
min	-1.58	-0.60	-0.33	-0.60		-2.18	-0.27	-0.22	-0.39	min	-0.55	-0.05	-0.02	-0.03	
median	0.01	-0.02	0.00	0.00		0.01	0.03	0.09	-0.01	median	0.00	0.00	0.00	0.00	
max	0.74	0.68	0.33	0.48		1.03	0.55	0.48	0.32	max	0.09	0.02	0.01	0.05	
skewness	-0.56	0.29	0.40	-0.49		-0.44	0.41	0.25	-0.21	skewness	-5.77	-0.22	0.05	-0.32	
kurtosis	1.99	1.03	0.07	0.16		1.85	-0.93	-0.29	-0.36	kurtosis	176.67	4.33	0.11	0.76	
$\rho(1)$	0.98	0.99	1.00	1.00		0.98	1.00	1.00	1.00	$\rho(1)$	0.77	0.92	0.99	0.96	
$\rho(6)$	0.94	0.96	0.98	0.97		0.94	0.99	0.98	0.97	$\rho(6)$	0.64	0.81	0.96	0.90	

This table presents summary statistics for the yield pricing errors from the long-short model and the ACM model. Panel A shows the errors from the long-short model, while Panels B and C show the results for the ACM model with K=2 and K=5 factors, respectively, where the latter follows the original specification by [Adrian et al. \(2013\)](#). For each model, we report the mean, standard deviation, skewness, and kurtosis of the errors, along with their first- and sixth-order autocorrelations, denoted by  $\rho(1)$  and  $\rho(6)$ . The statistics are calculated over the sample period from January 1987 to December 2025 for maturities of 0.25, 2, 5, and 10 years.

**Table 3: The Correlation between Implied  $R_t$  and  $L_t$** 

	Dependent Variable: $\Delta l_t$		
const	-0.001 [-0.41]	0.002 [0.70]	0.002 [0.80]
$\Delta r_t$	-0.18 [-1.26]		0.08 [0.76]
Dummy Hike		-0.01* [-1.74]	-0.004 [-0.95]
$\Delta r_t$ *Dummy Hike			-0.64** [-2.09]
N	9735	9735	9735
R2 (%)	0.25	0.03	0.98

This table reports the contemporaneous relationship between the daily change of  $r_t$  and  $l_t$ . Hike equals one when the Federal Reserve adopts a tightening policy during the period. A hiking period includes the first rate-increase meeting through the meeting immediately preceding the next rate cut.

**Table 4: Response of Implied Long and Short Yield to Monetary Policy Shocks**

Panel A: Dependent Variable= $r_t$								
const	-0.4 [-1.21]	-0.08 [-0.27]	0.11 [0.32]	0.24 [0.67]	0.2 [0.55]	0.15 [0.41]	-0.26 [-0.71]	-0.26 [-0.84]
Fed decision	0.10*** [2.77]							
Surprise		0.41*** [6.49]						
ED1			0.63*** [4.52]					
ED2				0.64*** [5.66]				
ED3					0.59*** [6.59]			
ED4						0.58*** [7.24]		
GSS target							0.46*** [3.02]	
GSS path								0.34*** [4.08]
N	263	211	263	263	263	263	234	234
R2 (%)	8.38	32.02	21.76	26.31	26.44	25.55	5.87	22.87
Panel B: Dependent Variable= $l_t$								
const	-1.87 [-1.48]	-0.74 [-0.62]	-2.24 [-1.46]	-2.05 [-1.30]	-1.85 [-1.16]	-1.68 [-1.05]	-2.66* [-1.83]	-2.66* [-1.80]
Fed decision	-0.30*** [-3.81]							
Surprise		-0.52*** [-4.43]						
ED1			-0.24 [-0.65]					
ED2				0.02 [0.06]				
ED3					0.24 [0.71]			
ED4						0.47 [1.52]		
GSS target							-0.29 [-0.81]	
GSS path								0.28 [0.95]
N	263	211	263	263	263	263	234	234
R2 (%)	7.98	3.88	0.31	0	0.45	1.7	0.23	1.38

This table reports estimated regression coefficients from FOMC-announcement-day regressions of latent  $r_t$  in Panel A and  $l_t$  in Panel B on the Fed decision and different monetary policy shocks. Fed decision is the actual monetary decision announced at scheduled FOMC meetings. Surprise is the unexpected component of the Fed decision calculated by [Kuttner \(2001\)](#). ED1-ED4 are changes in the first four quarterly Eurodollar futures contracts around FOMC announcements in [Bauer and Swanson \(2022\)](#). GSS Target and GSS Path are the monetary shocks from [Gurkaynak et al. \(2005\)](#).

**Table 5: Financial Market Responses to Latent and Observed Rates**

Panel A: Latent Factors							
	SPX	DXY	VIX	MOVE	MOVE <sup>⊥</sup>	EPU	Noise
const	0.03*** [2.95]	0 [-0.13]	0 [-0.10]	0 [-0.11]	0 [0.06]	-8.46*** [-17.84]	0 [-0.16]
$\Delta l_t$	0.61*** [4.69]	0.23*** [5.23]	-1.23*** [-6.86]	3.53*** [7.74]	4.32*** [9.89]	11.84*** [2.60]	0.03 [0.78]
$\Delta r_t$	1.89*** [3.85]	1.03*** [7.05]	-3.86*** [-5.49]	-2.82 [-1.30]	-0.09 [-0.04]	0.1 [0.01]	-0.58*** [-3.82]
N	9735	9734	8985	9422	8985	9736	9231
R2 (%)	1.38	1.75	2.65	2.4	3.64	0.09	0.58
Panel B: Constant Maturity Yield							
	SPX	DXY	VIX	MOVE	MOVE <sup>⊥</sup>	EPU	Noise
const	0.03*** [2.98]	0 [-0.14]	0 [-0.08]	0 [-0.10]	0 [0.08]	-8.46*** [-17.85]	0 [-0.15]
$\Delta CMT_t^{(10)}$	1.92*** [4.36]	0.68*** [5.01]	-4.29*** [-7.33]	9.82*** [6.47]	12.99*** [9.13]	37.43*** [2.63]	0.11 [0.95]
$\Delta CMT_t^{(3m)}$	1.19** [2.23]	0.30** [2.22]	-0.9 [-1.19]	-6.20*** [-3.44]	-5.91*** [-3.31]	-51.23*** [-3.17]	-0.86*** [-4.80]
N	9735	9734	8984	9421	8984	9736	9230
R2 (%)	1.53	1	2.5	1.87	3.35	0.16	1.31

This table reports coefficients from daily time-series regressions of financial and policy-market variables on interest-rate changes. In Panel A, the explanatory variables are changes in latent long-term and short-term factors from the long-short model,  $\Delta l_t$  and  $\Delta r_t$ . In Panel B, the explanatory variables are changes in Treasury constant-maturity 10-year and 3-month yields,  $\Delta CMT_t^{(10)}$  and  $\Delta CMT_t^{(3m)}$ . The dependent variables are the S&P 500 log return in percent (SPX), first differences of the U.S. dollar index (DXY), VIX, MOVE, the orthogonalized MOVE component MOVE<sup>⊥</sup>, the daily Economic Policy Uncertainty index (EPU), and the Treasury-market noise measure (Noise). The orthogonalized MOVE column is the residual from regressing the MOVE first difference on the VIX first difference in the daily regression sample. T-statistics are based on standard errors that are Newey-West (1987) adjusted with 4 lags, and are reported in brackets.

**Table 6: Inflation, Unemployment, and Interest Rates**

<b>Panel A: Macroeconomic Fundamentals</b>				
	$CMT_t^{(3m)}$	$CMT_t^{(10)}$	$r_t$	$l_t$
const	2.30*** [2.65]	1.42* [1.68]	2.66*** [3.06]	-2.29 [-1.29]
CPI Core	1.06*** [4.03]	0.98*** [3.99]	1.08*** [4.31]	1.31*** [3.43]
Unemployment	-0.37*** [-4.60]	0.08 [0.79]	-0.44*** [-5.17]	0.81*** [3.00]
N	467	467	467	467
R2 (%)	40.04	26.40	43.03	18.92
<b>Panel B: Daily Market-Based Inflation Expectations</b>				
	$\Delta CMT_t^{(3m)}$	$\Delta CMT_t^{(10)}$	$\Delta r_t$	$\Delta l_t$
const	0 [0.71]	0 [-0.09]	0 [0.86]	0 [-0.42]
$\Delta 5YBEI$	0.12*** [3.44]	0.37*** [11.02]	0.09*** [3.15]	1.03*** [9.58]
$\Delta 5Y5YBEI$	0.06** [2.10]	0.38*** [13.16]	0.02 [0.88]	1.05*** [11.14]
N	5753	5753	5753	5753
R2 (%)	2.00	19.81	1.00	14.47

This table reports regressions of observed Treasury constant-maturity yields and latent factors from the long-short model on macroeconomic fundamentals and market-based inflation expectations. Panel A uses monthly data. The dependent variables are the 3-month and 10-year Treasury constant-maturity yields,  $CMT_t^{(3m)}$  and  $CMT_t^{(10)}$ , the latent short-rate factor  $r_t$ , and the latent long-rate factor  $l_t$ . The explanatory variables are core CPI inflation, measured year over year, and the unemployment rate, both measured in percent. Panel B uses daily first differences. The dependent variables are changes in the same two Treasury constant-maturity yields and latent factors. The explanatory variables are daily changes in the 5-year breakeven inflation rate and the 5-year, 5-year forward breakeven inflation rate. T-statistics are based on standard errors that are Newey-West (1987) adjusted with 4 lags, and are reported in brackets. Panel A covers January 1987 to December 2025; Panel B uses the daily sample with available breakeven inflation and latent-factor changes.

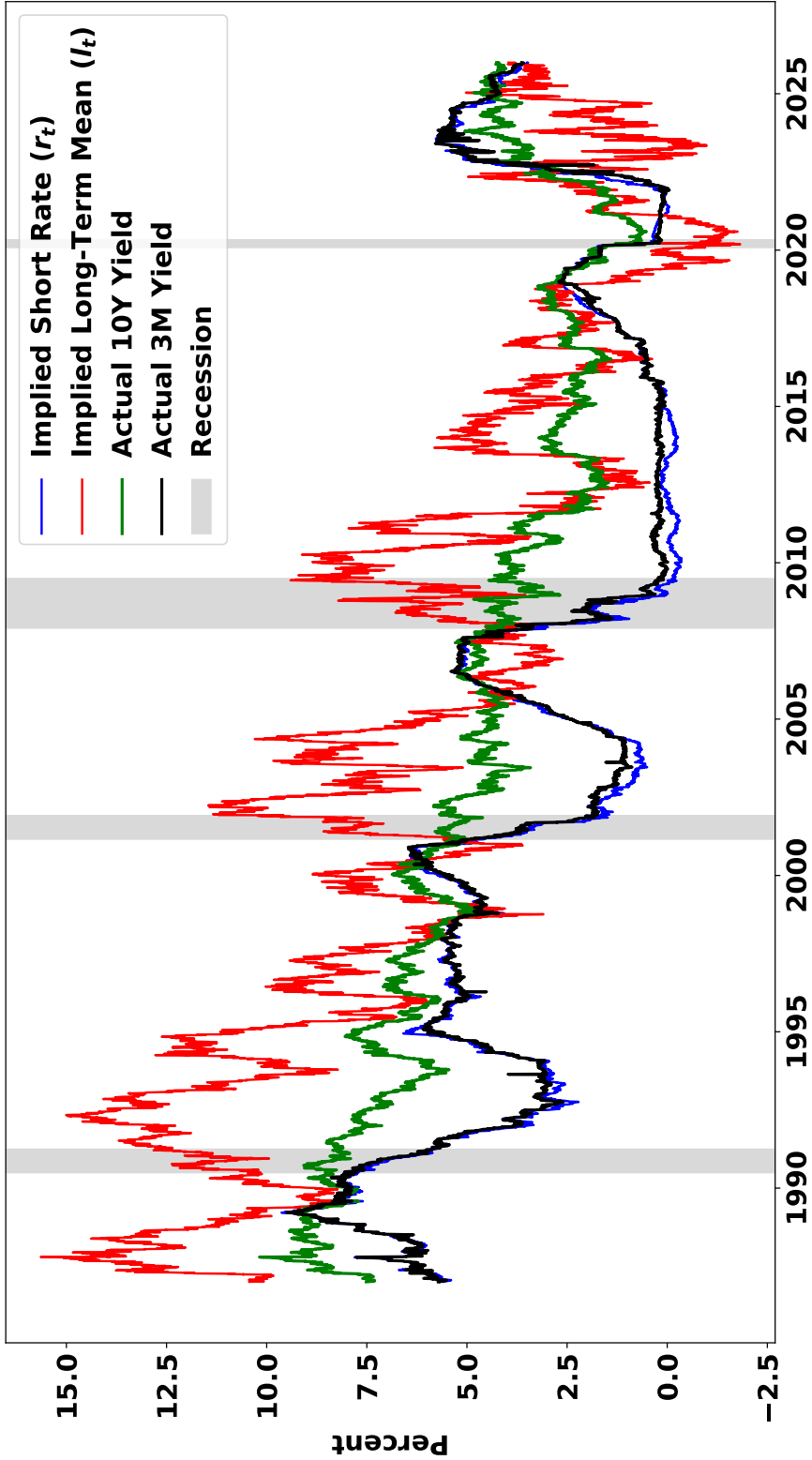
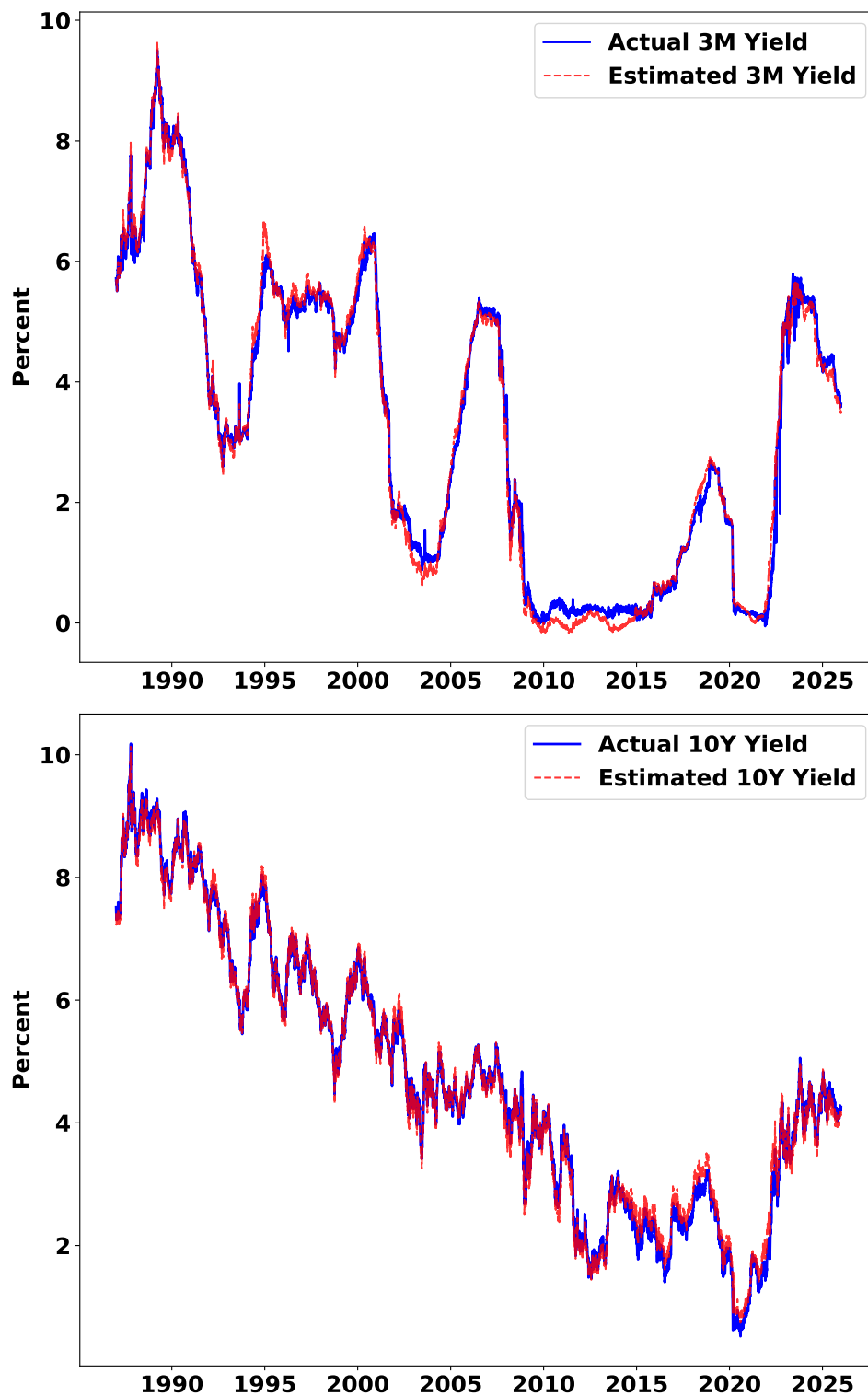
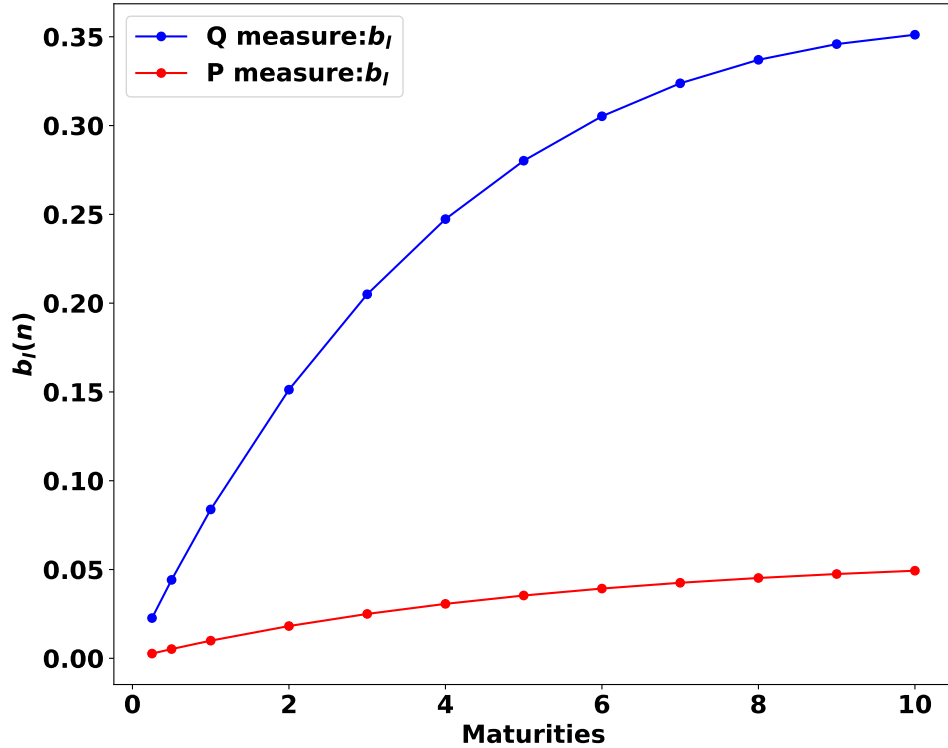
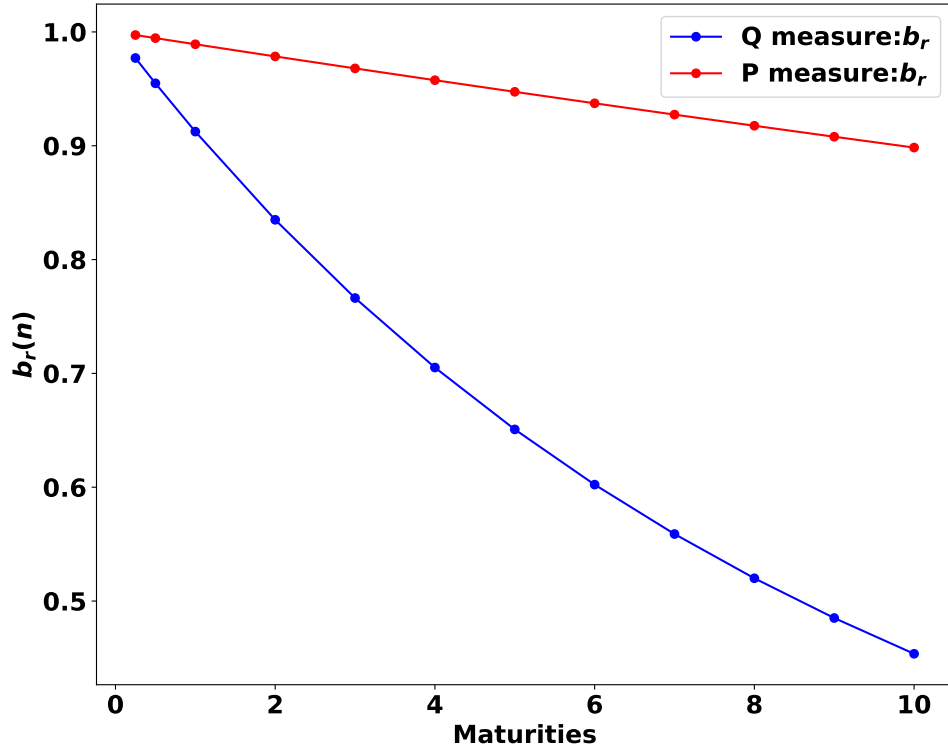


Figure 1: Implied State Variables from the Long-Short Model and Actual Yields. This figure plots the implied  $r_t$  in blue and  $l_t$  in red extracted from the long-short model over the period from January 1987 to December 2025. The actual 3-month and 10-year yields are also plotted. The shaded areas are NBER recession periods.



**Figure 2: Observed and Model-Implied Time Series.** The figure shows time series of yields for 3-month and 10-year maturities as observed and implied by the long-short model. The actual yields are plotted as solid blue lines, and dashed lines correspond to model-implied yields.



**Figure 3: Factor Loadings  $b(n)$ .** This figure plots the coefficients  $b(n)$  from Eq. 8 for different maturities. The upper panel plots the coefficient associated with the latent  $r_t$  factor; the blue line is calculated using the parameters under the  $\mathbb{Q}$  measure, while the red line uses the parameters under the  $\mathbb{P}$  measure. The lower panel plots the coefficient associated with the latent  $l_t$  factor.

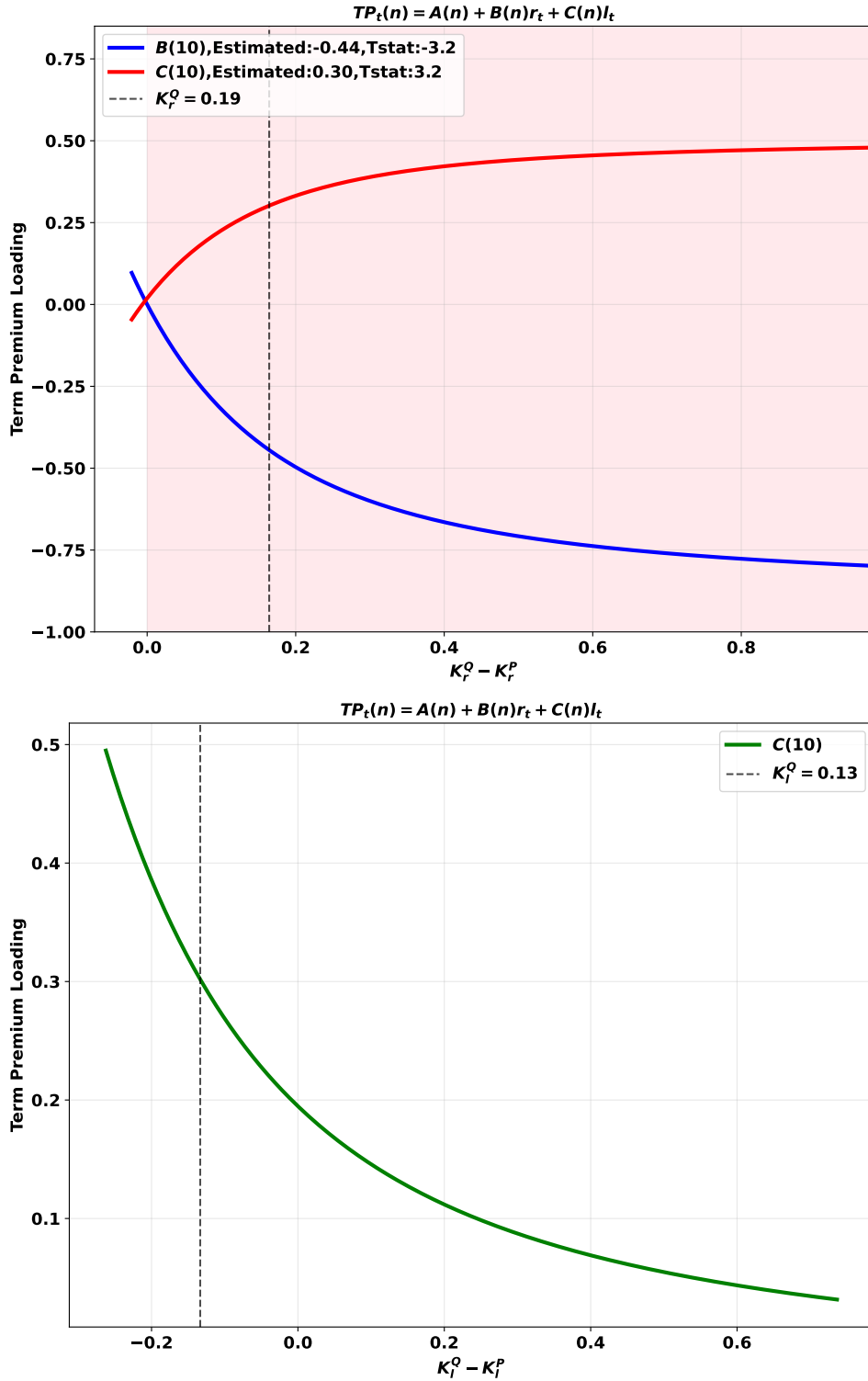


**Figure 4: Term Premium Loading  $B(n)$  and  $C(n)$ .** This figure plots the coefficients  $B(n)$  and  $C(n)$  from Eq. (12). The upper figure shows how the 10-year term-premium loadings vary with the difference  $K_r^Q - K_r^P$ . The blue line is  $B(n)$  for 10-year maturity under a fixed physical-measure parameter  $K_r^P = 0.02$  while varying the risk-neutral parameter  $K_r^Q$ . The red line is  $C(n)$  for 10-year maturity with fixed baseline  $K_r^P = 0.02$ ,  $K_l^P = 0.26$ ,  $K_l^Q = 0.13$  and varying only  $K_r^Q$ . The vertical dashed line marks the value  $K_r^Q = 0.19$  used in our baseline estimation. The lower figure shows how the coefficient  $C(10)$  varies with the difference  $K_l^Q - K_l^P$ . The green line is  $C(n)$  for 10-year maturity with fixed baseline  $K_r^P = 0.02$ ,  $K_l^P = 0.26$ ,  $K_r^Q = 0.19$  and varying only  $K_l^Q$ .

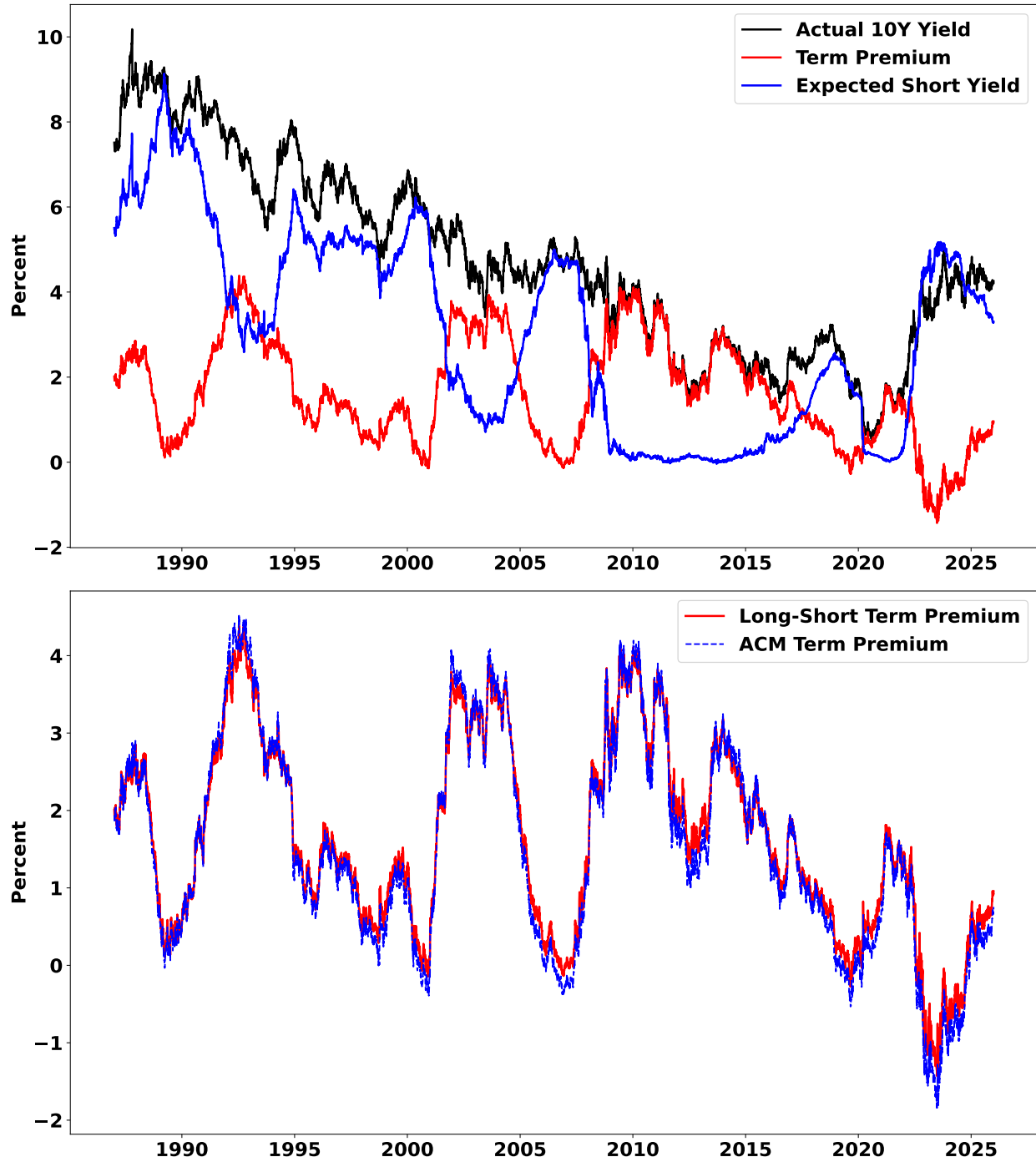


**Figure 5: Yield Decomposition and Estimated Term Premium.** The upper figure decomposes the observed 10-year yield into the expected short-rate component in blue and the term premium in red. The lower figure compares the 10-year term premium estimated from the long-short model in solid red and the ACM method ([Adrian et al., 2013](#)) in dashed blue.

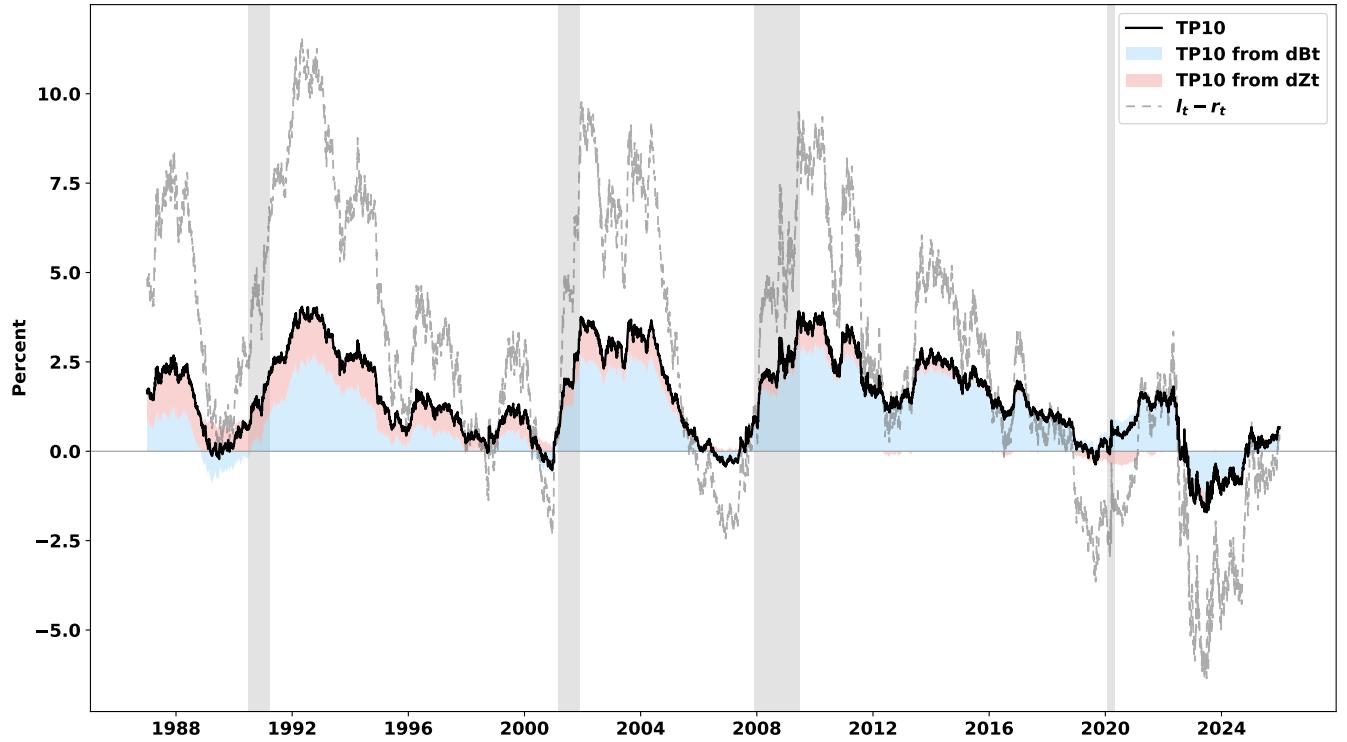


**Figure 6: Term Premium Decomposition.** This figure decomposes the 10-year term premium into contributions from  $dB_t$  and  $dZ_t$  risks. The black line is the full term premium. The blue area captures the contribution from  $dB_t$  risk, while the red area captures the residual contribution from  $dZ_t$  risk. The dashed gray line shows the spread between latent long rate and short rate from the long-short model.

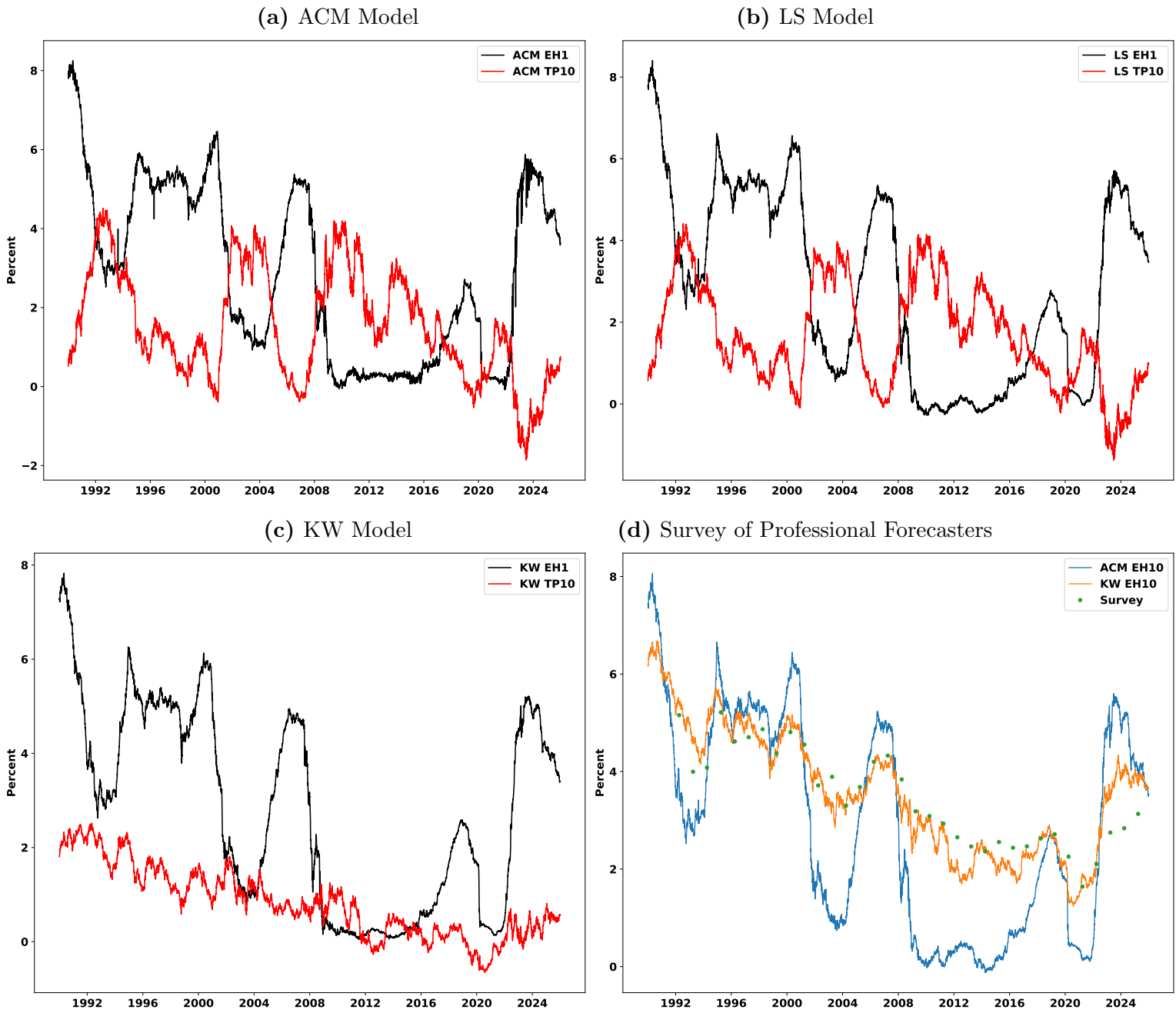


**Figure 7: The Comovement between Short-Rate Expectations and Term Premium.** The figure plots the time series of short-rate expectations and term premia from the ACM model in Panel A, from the long-short model in Panel B, and from the KW model in Panel C. Average expected short rates from the Survey of Professional Forecasters, as well as from the ACM and KW models, over 10 years are plotted in Panel D.

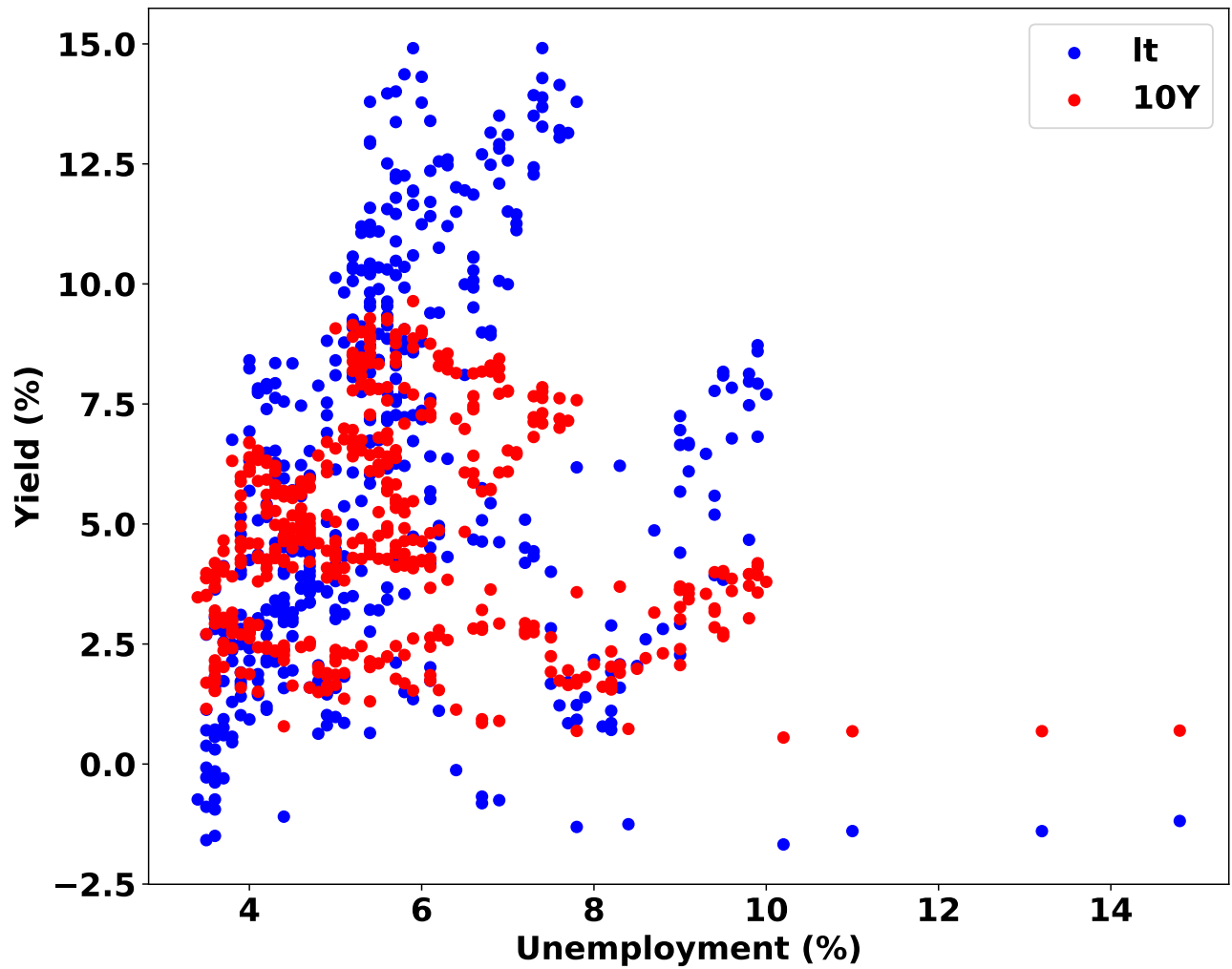


**Figure 8: The Unemployment Rate and Long-Term Rate** The unemployment rate is plotted against the latent long-term rate  $l_t$  from the long-short model in blue and the observed 10-year rate in red.